Biochimica et Biophysica Acta 1803 (2010) 246–260

Contents lists available at ScienceDirect

Biochimica et Biophysica Acta

journal homepage: www.elsevier.com/locate/bbamcr

Influence of spontaneous calcium events on cell-cycle progression in embryonal carcinoma and adult stem cells

R.R. Resende [a,b,c,*], A. Adhikari [d], J.L da Costa [e], E. Lorençon [a], M.S. Ladeira [f], S. Guatimosim [f], A.H. Kihara [g], L.O. Ladeira [a]

[a] Department of Physics, Institute of Exact Sciences, Federal University of Minas Gerais, Belo Horizonte, MG 31270-901, Brazil
[b] Institute of Learning and Research Santa Casa of BH (IEPSC-BH), Belo Horizonte, Brazil
[c] Federal University of São João Del-Rei-Campus Centro-Oeste, Divinópolis-MG, Brazil
[d] Department of Biological Sciences, Columbia University, New York, NY 10027, USA
[e] Instrumental Analysis Laboratory, Criminalistic Institute of São Paulo, SP, Brazil
[f] Department of Physiology and Biophysics, Institute of Biological Sciences, Federal University of Minas Gerais, Belo Horizonte, MG 31270-901, Brazil
[g] Núcleo de Cognição e Sistemas Complexos-Centro de Matemática, Computação e Cognição-Universidade Federal do ABC, Santo André, SP, Brazil

ARTICLE INFO

Article history:
Received 10 June 2009
Received in revised form 28 October 2009
Accepted 18 November 2009
Available online 1 December 2009

Keywords:
Mesenchymal stem cell
P19 embryonic carcinoma stem cell
Neuronal differentiation
Calcium signaling
Cell cycle
Spontaneous calcium oscillation

ABSTRACT

Spontaneous Ca^{2+} events have been observed in diverse stem cell lines, including carcinoma and mesenchymal stem cells. Interestingly, during cell cycle progression, cells exhibit Ca^{2+} transients during the G_1 to S transition, suggesting that these oscillations may play a role in cell cycle progression. We aimed to study the influence of promoting and blocking calcium oscillations in cell proliferation and cell cycle progression, both in neural progenitor and undifferentiated cells. We also identified which calcium stores are required for maintaining these oscillations. Both in neural progenitor and undifferentiated cells calcium oscillations were restricted to the G1/S transition, suggesting a role for these events in progression of the cell cycle. Maintenance of the oscillations required calcium influx only through inositol 1,4,5-triphosphate receptors (IP_3Rs) and L-type channels in undifferentiated cells, while neural progenitor cells also utilized ryanodine-sensitive stores. Interestingly, promoting calcium oscillations through IP_3R agonists increased both proliferation and levels of cell cycle regulators such as cyclins A and E. Conversely, blocking calcium events with IP_3R antagonists had the opposite effect in both undifferentiated and neural progenitor cells. This suggests that calcium events created by IP_3Rs may be involved in cell cycle progression and proliferation, possibly due to regulation of cyclin levels, both in undifferentiated cells and in neural progenitor cells.

Published by Elsevier B.V.

1. Introduction

Cell cycle progression in mammalian somatic cells is known to be dependent on intracellular Ca^{2+} signaling [1,2]. Accordingly, previous reports showed that spontaneous Ca^{2+} events were observed in the G_0/G_1 phases of the cell cycle, suggesting a possible role for these events in reentry into the cell cycle [3]. Furthermore, G_1/S and G_2/M transitions are also coupled to increases in spontaneous Ca^{2+} oscillations, which were demonstrated to be dependent on inositol 1,4,5-triphosphate receptors, (IP_3Rs) [2,4].

Cell cycle progression is known to require Ca^{2+} influx from both extra- and intracellular sources. Accordingly, calcium removal from the extracellular solution and inhibition of replenishment of endoplasmic reticulum (ER) calcium stores result in arrest of the cell cycle in the G_1/S transition [5,6]. Calcium influx from internal (through ryanodine receptors and IP_3Rs) and external stores (via store-operated Ca^{2+} channels and voltage gated calcium channels) are involved in cell proliferation [5,7–12].

Calcium wave-signaling is widespread, as it has been observed in cortical radial glia, in the ventricular zone [7,8], neurospheres [9], mesenchymal stem cells [10,13], mouse embryonic stem cells [11], mouse carcinoma stem cells [13] and cells in developing tissue [12,14–16]. Although calcium oscillations have been observed in numerous model systems, many questions about the role of these Ca^{2+} events in cell cycle progression and cellular proliferation remain unanswered. For instance, it is not known if the calcium stores necessary to maintain these calcium events are the same in embryonic and adult stem cells, or if they are conserved across neuronal differentiation. The mechanisms through which calcium events regulate cellular proliferation and progression of the cell cycle are also unknown. In the present work, to investigate these issues, we studied calcium oscillations throughout the cell cycle in undifferentiated and neural progenitor cells (NPCs), and identified which calcium stores are necessary for the occurrence of these oscillations.

* Corresponding author. Department of Physics, Institute of Exacts Sciences, Federal University of Minas Gerais, Av. Antônio Carlos, 6627, 31270-901, Belo Horizonte, MG, Brazil. Tel.: +55 31 3409 5614; fax: +55 31 3409 5616.
E-mail addresses: rrresende@hotmail.com, resende@santacasabh.org.br (R.R. Resende).

0167-4889/$ – see front matter. Published by Elsevier B.V.
doi:10.1016/j.bbamcr.2009.11.008

We also studied the effects of manipulating calcium oscillations on proliferation and progression of the cell cycle. To this end we used stem cells derived from embryonic (P19 embryonic carcinoma stem cells, or CSCs) and adult tissue (murine bone-marrow derived mesenchymal stem cells, or MSCs). We show that calcium events are regulated by IP_3Rs in undifferentiated stem cells and by IP_3Rs and ryanodine receptors (RyRs) in neural progenitor cells. Interestingly, spontaneous Ca^{2+} oscillations were restricted to the G_1/S phase transition of the cell cycle, suggestive of a role for these oscillations in cell cycle progression. Lastly, blocking calcium oscillations with IP_3R antagonists decreased proliferation and blocked progression of the cell cycle, while promoting calcium oscillations with IP_3Rs agonists had the opposite effect, both in CSCs and MSCs. Importantly, we demonstrate that IP_3R-mediated pathways modulate proliferation and progression of the cell cycle in a similar fashion in both undifferentiated cells and neural progenitor cells. We also show that the previously reported association between IP_3Rs and proliferation [17] may be due to an IP_3R-mediated increase in the expression levels of cyclins A and E. Thus, our data show that IP_3Rs regulate both the cell cycle and calcium oscillations. These findings support a possible role for calcium oscillations in progression of the cell cycle. These effects were observed in both stem cells and neural progenitor cells derived from embryonic carcinoma and adult stem cells, suggesting it may be a conserved mechanism for stem cells from different origins.

2. Materials and methods

2.1. Reagents

Unless indicated otherwise, all reagents were purchased from Sigma (St. Louis, MO). Primers for Real Time PCR reactions were synthesized by Integrated DNA Technologies (Coralville, IA). The following antibodies were used for immunoprecipitation and Western blots: sc-601-G against CDK4, sc-163-G against CDK2, sc-177 against CDK6, sc-751 against cyclin A, sc-481 against cyclin E (all purchased from Santa Cruz Biotechnology); mouse monoclonal antibody to mouse p27 (K25020) (Transduction Laboratories, Lexington, KY); mouse monoclonal antibodies against cyclin A (Ab-1, E23) and cyclin D2 (Ab-4, DCS-3.1 + DCS-5.2) [18] (Abcam, Cambridge, UK); mouse monoclonal antibody against the C-terminal of human cyclin D3, which cross-reacts with the mouse homologue (DCS-22) [19]. Anti-nestin (Chemicon International Inc., Temecula, CA), anti-NEL (Santa Cruz Biotechnology, Delaware, CA) and secondary antibodies coupled with cytochrome 3 (Cy3, 1:200, Jackson Immunoresearch, West Grove, PA). The following polyclonal rabbit antisera were used: anti-nestin, anti-neuronal enolase (NEL), anti-SSEA-1 (Santa Cruz Biotechnology, Heidelberg, Germany) and anti-β-actin.

2.2. Culture and neuronal differentiation of CSC cells

P19 embryonic carcinoma cells (CSCs) cells (*kindly* provided by Prof. Dr. José Garcia Ribeiro Abreu Jr., ICB, UFRJ) were maintained in Dulbecco's modified Eagle's medium (DMEM, Invitrogen, Carlsbad, CA) supplemented with 10% fetal bovine serum (FBS, Cultilab, Campinas, Brazil), 100 units/ml penicillin, 100 μg/ml streptomycin, 2 mM L-glutamine, and 2 mM sodium pyruvate and in a humidified incubator at 5% CO_2 and 37 °C. For neuronal differentiation induction experiments, cells were exposed to 1 mM of *all trans*-retinoic acid (RA). Formation of embryonic bodies (EBs) was induced by culturing P19 cells in suspension in bacterial culture dishes coated with 0.2% agarose for 48 h at a density of 5×10^5 cells/ml in defined serum-free medium as described previously [20–23]. The medium was changed every 2 days after plating on bacterial dishes. Eight days following addition of RA, neuronal differentiation was completed, as confirmed by immunostaining against neuronal proteins NF-200, neuron-specific enolase, and β-3-tubulin (data not shown). Differentiated P19 cell cultures were kept free from glial cells by treatment with 50 μg/ml cytosine arabinoside on the 6th day after induction of differentiation [20–22].

2.3. Isolation and culture of sphere-derived cells from murine bone marrow (MSCs)

All experiments were performed in accordance with the Animal Protection Guidelines of the Federal University of Minas Gerais. Bone marrow cells (MSCs) were collected from 2-month-old C57Bl/6 mice bone marrow cells (MSCs) as previously described [13,24]. Femurs and tibias from mice were flushed with complete medium constituted of DMEM, 10% fetal calf serum (FCS, Sigma), 100 U/ml penicillin, 100 mg/ml streptomycin, 2 mM glutamine, and 5 U/ml heparin. Cells were then plated at a density of 2×10^6 cells/cm^2. Immunomagnetic separation with Dynabeads, in accordance to the manufacturer's protocol was used to separate differentiated hematopoietic cells. Briefly, primary rat anti-mouse antibodies, anti-CD8, CD11b, CD4, CD45R/B220, Ter119, and Gr 1 (PharMingen, San Jose, CA), were used to stain MSCs. Labeled cells were removed using Dynabeads M-450 Sheep anti-Rat IgG (Dynal Biotech, Oslo, Norway) with a Dynal Magnetic Particle Concentrator (Dynal Biotech) by centrifugation. The supernatant containing the lineage-depleted MSCs was then collected. Immunodepleted MSCs were resuspended in 10 ml of complete medium and plated on a 35×10 mm tissue culture dish (NUNC, Naperville, IL). Cells were cultured in a humidified incubator containing 5% CO_2 and 5% O_2 at 37 °C for 24 h, non-adherent cells were removed and fresh complete medium was added. Cells were cultured until they reached 70–80% confluency and then adherent cells were detached with trypsin/EDTA and plated on 35×10 mm standard tissue culture dishes.

2.4. MSC sphere formation and culture expansion

A total of 100,000 cells were suspended in complete medium on dishes coated with 0.2% agarose. Suspended cells formed spheres and gradually increased in size. Seven days after suspension, cells were dissociated mechanically by gentle pipetting. Dissociated cells were cultured in complete medium, which was changed every other day. After reaching 40–50% confluency, cells were detached with Trypsin/EDTA and replated at a 1:4 dilution. Sphere-derived cells were harvested for the experiments as described below when each well contained more than 1×10^7 cells.

To induce neuronal differentiation, sphere-derived cells were treated as previously described [13,24]. Briefly, cells were plated at a cell density of 1×10^4 cells/cm^2 on gelatin-coated dishes in neurobasal medium (Gibco BRL) with B27 Supplement (50×, Invitrogen), 20 ng/ml EGF, and 10 ng/ml bFGF for 7 days, followed by culture in neurobasal medium with 0.5 μM retinoic acid and 20 ng/ml β-NGF for 5 days.

Experiments were performed on control cultures the first day after plating. Pharmacological synchronization of cells in specific phases of the cell cycle was started 24 h after plating, and cells were incubated for a minimum of 12 h before experimental use.

2.5. Calcium oscillation analysis in CSC and MSC cells

CSC and MSC cells were loaded with Fluo3-AM by incubation with 4 μM Fluo3-AM in 0.5% Me_2SO and 0.1% of the non-ionic surfactant pluronic F-127 for 30 min at 37 °C in an extracellular medium containing 140 mM NaCl, 3 mM KCl, 1 mM $MgCl_2$, 2.5 mM $CaCl_2$, 10 mM HEPES, and 10 mM glucose at pH 7.4. After loading with Fluo3-AM, cells were washed with incubation buffer and incubated for 20 min to ensure complete de-esterification of Fluo3-AM. Ca^{2+} imaging was performed with an LSM 510 confocal microscope (Zeiss, Jena, Germany) at 20–22 °C. Fluo3 was excited with a 488 nm line

from an argon ion laser and the emitted light at 515 nm was detected using a band pass filter. At the end of each experiment, 5 μM of the ionophore 4-Br-A23187 followed by application of 10 mM EGTA were used to determine maximal (F_{max}) and minimal (F_{min}) fluorescence values. Ca^{2+} concentration was calculated from the Fluo3 fluorescence emission using a self-ratio equation as described previously [13,20,21,25], assuming a K_d of 450 nM. The osmolarity of all the solutions ranged between 298 and 303 mosmol/L. Calcium concentrations were calculated for cell populations of at least 10 cells in three different experiments. Calcium oscillations from neural progenitor cells derived from both CSCs and MSCs were measured 6 days after the induction of neuronal differentiation. As we described previously [13,20], at this time point 31% and 32% of cells were neural progenitor cells, in CSCs and MSCs, respectively [13,20]. For measurements of calcium oscillations in neural progenitor cells cell identity was confirmed with immunofluorescence. Cells were incubated with anti-nestin (Chemicon International Inc.) or anti-NEL (Santa Cruz Biotechnology, Delaware, CA) antibody at 4 °C overnight. This was followed by incubation with secondary antibodies coupled to cytochrome 3 (Cy3, Jackson Immunoresearch) at room temperature (RT) for 1 h. All calcium oscillation data from neural progenitor cells are from cells that express nestin or NEL.

To evaluate the contribution of extracellular and intracellular Ca^{2+} mobilization to Ca^{2+} oscillations, the effects of various drugs were studied. To study the influence of external calcium on calcium oscillations, cells were treated with the extracellular calcium chelator EGTA (1 mM). The effect of inhibitors of the sarcoplasmatic/endoplasmatic reticulum Ca^{2+}-ATPase (SERCA) such as cyclopiazonic acid (CPA, 10 μM) [13,25] and 1 μM thapsigargin [26] on oscillations were evaluated to study the role of depleting ER calcium on calcium events. The influence of voltage-gated calcium channels (VGCC) on oscillations was also studied. To this end, cells were exposed to the VGCC blocker $CdCl_2$ (100 μM) [27] and to the L-type calcium blocker nifedipine (5 μM) [27,28] and an agonist of L-type channels Bay-K (10 μM). In order to investigate the influence of store operated Ca^{2+} channels (SOCs) on calcium oscillations, the SOC inhibitor lanthanum (50 μM) was used [29–31]. 2-Aminoethoxydiphenyl borate (2-APB, 10 μM), a cell permeant and reversible inhibitor of IP_3R opening [32] was used to study the involvement of IP_3Rs on oscillations. Ryanodine (10 μM; Rya InhC), which at this concentration act as an inhibitor of RyR [33], was used to study the involvement of RyRs on calcium oscillations. The effect of caffeine (10 mM) was also studied, for caffeine at this concentration acts both as an inhibitor of the IP_3R [34] and as an activator of RyRs [35]. Various drugs were used to evaluate the contribution of IP_3Rs on calcium oscillations, such as U-73122 (5 μM), a phospholypase C inhibitor [36], and xestospongin C (XeC) (1 μM), a membrane-permeable inhibitor of IP_3 [28]. XeC at 1 μM only affects the IP_3R, but not the RyR, which has an $IC_{50} = 22.6 \pm 2.2$ μM [37]).

To evaluate the contribution of extracellular and intracellular Ca^{2+} mobilization on cell growth rate and cell cycle progression, the effects of 5 μM U-73122, a phospholypase C inhibitor and its biologically inactive analog U-73343 (5 μM) [36] were evaluated. The effect of the intra-cellular calcium chelator BAPTA-AM (10 μM) was also studied. Growth rate and cell cycle analysis assays were also carried out in the presence of thapsigargin (1 μM) [26], XeC (1 μM) [28], nifedipine (5 μM) and lanthanum (50 μM), IP_3R influence on cell growth was studied by exposing cells to the reversible inhibitor of IP_3R opening 2-aminoethoxydiphenyl borate (2-APB, 10 μM) [32], the IP_3R agonist adenophostin-A (AdA) (2 nM) [38,39], and thimerosal (10 μM), a thiol reagent described to increase the sensitivity of IP_3R for its agonist [40].

2.6. Immunocytochemical analysis of the cell cycle

After recording calcium transients, a mark was made by a needle around the cell on the slide (Lab-Tek). Cells were rapidly fixed in −20 °C ethanol (75%) for 30 min and subsequently washed with and incubated in phosphate-buffered solution containing 1 mg/ml bovine serum albumin for 10 min at 25 °C. Double-labeled immunofluorescence staining was carried out by incubation with monoclonal antibodies against cell cycle-specific nuclear antigens (fluorescein isothiocyanate-conjugated anti-PCNA and *R*-phycoerythrin-conjugated Ki-67) for 30 min at 25 °C. Stained cells were observed under a fluorescence microscope (Axioskop, Zeiss) and photographed for later analysis. PCNA expression varies throughout the cell cycle, as it has no expression in the G_0 phase, moderate expression in the G_1 or G_2 phase, and maximal expression in the S phase. Ki-67 expression also differs in different phases of the cell cycle, as it has no expression in the G_0 phase, weak and aggregated expression in the G_1 phase, increasing expression in the S phase, and maximal expression in the G_2 and M phases. Thus, double staining with these two markers results in a different nuclear fluorescence color for each phase of the cell cycle. Cells in G_0 had no specific nuclear fluorescence, whereas the cells in G_1 showed green fluorescence (PCNA) associated with aggregated spotty red-orange fluorescence (Ki-67). Cells in the M phase had red (Ki-67) fluorescence, and cells in the S phase emitted both red (Ki-67) and green (PCNA) fluorescence, thus giving them a yellow appearance. Double staining coupled allowed to identify the cell cycle phase of the cell enclosed by the mark made by the needle. Differential nuclear staining was confirmed in stem cells by arresting cells in the S or M phase with aphidicolin and TN-16, respectively.

2.7. Cell cycle synchronization and detection by fluorescence-activated cell sorting

To synchronize CSCs and MSCs in the transition from G_1 to S phase, cells were incubated for 12 h with mimosine (MIM; 500 μM), an inhibitor of the cell cycle which induces arrest in G_1 by chelating iron ions and inhibiting DNA replication in mammalian cells [41] or hydroxyurea (HU; 2 mM), which blocks the synthesis of deoxynucleotides inhibiting DNA synthesis, inducing synchronization in S-phase [42]. In order to synchronize cells in the transition from G_2 to M, cells were treated with demecolcine (DC; 20 ng/ml), which arrests cells in metaphase [43]. Nocodazole (NOC; 100 ng/ml), was used to arrest the cell cycle at G_2/M phase, as this drug disrupts mitotic spindles [44]. After 12 h, the cells were washed with EM and used for Ca^{2+} imaging experiments within 2 h. Cell cycle distribution was determined using a FACS Calibur flow cytometer (Becton Dickinson, San Jose, CA). Cells were washed with phosphate buffered saline and incubated for 10 min in ice-cold ethanol (70%). After washing, cells were treated with RNase (100 mg/million cells in PBS; 30 min at 37 °C). Propidium iodide (PI, 50 μg/ml)/RNase A staining buffer was added for 60 min at 4 °C. PI fluorescence was detected at 600 nm by exciting at 488 nm. Data were acquired with Cell Quest software, and the percentages of G_1, S, and G_2 phase cells were calculated with MODFIT software.

2.8. RNA isolation, reverse transcription and real-time PCR

Total RNA was isolated using TRIzol (Invitrogen) from undifferentiated CSC and MSC cells. Integrity of the isolated RNA was verified by separation on a 2% ethidium bromide-stained agarose gel. DNA was removed from RNA samples by incubation with DNase I (Ambion Inc., Austin, TX). Primer sequences for reverse transcription and PCR amplification of β-actin, IP_3Rs and RyRs isoforms mRNA are listed in Table 1. Negative controls were treated with water and total RNA was non-reverse transcribed. DNA templates were amplified by real time PCR on the 7000 Sequence Detection System (ABI Prism, Applied Biosystems, Foster City, CA, USA) using the Sybr green method [20,21,45]. β-Actin was used as an internal control to normalize variations in cDNA concentrations. Experiments were performed in triplicate for each data point. After amplification, electrophoresis of

Table 1
Primers for amplification of $InsP_3Rs$ and RyRs receptors subtypes by real time PCR. FWD = forward primer; REV = reverse primer.

Gene	Access number	Primer	Sequence (5′–3′)	Length (bp)
qRT-PCR				
IP3R1	NM_010585	FWD	5′ CTGCTGGCCATCGCACTT 3′	66
		REV	5′ CAGCCGGCAGAAAAACGA 3′	
IP3R2	NM_019923	FWD	5′ AGCACATTACGGCGAATCCT 3′	77
	NM_0105868	REV	5′ CCTGACAGAGGTCCGTTCACA 3′	
IP3R3	NM_080553	FWD	5′ CGGAGCGCTTCTTCAAGGT 3′	75
		REV	5′ TGACAGCGACCGTGGACTT 3′	
RYR1	NM_009109	FWD	5′ AGACGCTACCACCGAGAAGAAC 3′	83
		REV	5′ TGGAAGGTGGTTGGGTCATC 3′	
RYR2	NM_023868	FWD	5′ CCGCATCGACAAGGACAAA 3′	76
		REV	5′ TGAGGGCTTTTCCTGAGCAT 3′	
RYR3	NM_177652	FWD	5′ CGCCTGAGCATGCCTGTT ′3	93
		REV	5′ TTCTTGCATCTGTTTCCTTTTTTG 3′	
β-Actin	NM_007393	FWD	5′ GACGGCCAGGTCATCACTATTG 3′	66
		REV	5′ AGGAAGGCTGGAAAAGAGCC 3′	

10 μl reaction mixture on a 2% NuSive/agarose gel (3:1) (FMC product, Rockland, ME) was visualized under UV illumination after staining with ethidium bromide.

2.9. Proliferation assays

To determine DNA synthesis rate, cells were exposed to 5-bromo-2-deoxyuridine (BrdU; Amersham Life Sci). Twenty-four hours prior to proliferation stimulation, undifferentiated and neural progenitor cells from both CSC and MSCs were kept in serum-free defined medium. Cells were then maintained for 12 h in culture medium in the absence or presence of the following drugs: U-73122 (5 μM) and its biologically inactive analog U-73343 (5 μM) [36], BAPTA-AM (10 μM), thapsigargin (1 μM) [26], 2-APB (10 μM) [32], XeC (1 μM) [28], nifedipine (5 μM), lanthanum (50 μM), AdA (2 nM) [38,39], and thimerosal (10 μM) [40]. BrdU (15 μM) was then added to the cell culture for 60 min. BrdU labeling was monitored and used as a measure for cell proliferation. To measure BrdU incorporation, cells were incubated with an anti-BrdU monoclonal antibody (Roche Applied Science, Indianapolis, IN) followed by incubation with biotinylated goat anti-mouse IgG and avidin–biotin complex (Jackson Immunoresearch; 1:200). Aminoethylcarbazole was used as a chromogen for visualization of BrdU-positive cells. A more detailed description of the method used can be found elsewhere [13,22].

For immunofluorescence double-labeling experiments, embryonic cells were fixed in acidic alcohol and processed for nestin staining, followed by BrdU incorporation and anti-BrdU staining. Cell preparations were then incubated with rabbit anti-nestin antibody (1:200; Chemicon International Inc.) and immunofluorescence was detected in the presence of anti-rabbit IgG-Cy3 (Abcam, Cambridge, MA) or IgG-Alexa-Fluor 488 (Molecular Probes, Eugene, OR) secondary antibodies. Incubations were performed for 1 h at room temperature. Nestin immunostaining was followed by incubation with 1 N HCl, neutralization with 0.1 M sodium tetraborate and incubation with Alexa Fluor 647-conjugated anti-BrdU (Molecular Probes) monoclonal antibodies for 1 h at room temperature. After washing with phosphate-buffered saline (PBS), BrdU/Nestin stained cells were examined by fluorescence microscopy.

2.10. Preparation of cytosolic and total membrane fractions

Cytosolic and total membrane fractions were prepared using a slight modification of the method reported by Mackman et al. [46]. Medium from undifferentiated and neural progenitor cells (NPCs) from the 4th day of differentiation of CSCs and MSCs was removed and replaced with serum-free DMEM including all the supplements contained in the defined medium for 12 h prior to the experiments. After removing the medium, cells were washed twice with ice-cold PBS, scraped, harvested by microcentrifugation, and resuspended in buffer A (137 mM NaCl, 8.1 mM Na_2HPO_4, 2.7 mM KCl, 1.5 mM KH_2PO_4, 2.5 mM EDTA, 1 mM dithiothreitol, 0.1 mM phenylmethylsulfonyl fluoride, 10 μg/ml leupeptin, 0.5 mM sodium orthovanadate, pH 7.5). Resuspended cells were then mechanically lysed on ice by trituration with a gauge needle. Cell lysates were initially centrifuged at 1000 × *g* for 10 min at 4 °C. Supernatants were collected and centrifuged at 100,000 × *g* for 1 h at 4 °C to prepare the cytosolic and total particulate fractions. The supernatant (cytosolic fraction) was then precipitated with five volumes of acetone, incubated in ice for 5 min, and centrifuged at 20,000 × *g* for 20 min at 4 °C. The resulting pellet was resuspended in buffer A, containing 1% (vol/vol) Triton X-100. The particulate fractions containing the membrane fraction were washed twice and resuspended in buffer A containing 1% (vol/vol) Triton X-100. Protein levels were quantified using Bradford's procedure [47].

2.11. Western blot analysis

Cells were harvested, washed twice with phosphate-buffered saline, and exposed to lysing buffer (20 mM Tris [pH 7.5], 1 mM EDTA, 1 mM EGTA, 1% Triton X-100, 1 mg/ml aprotinin, 1 mM phenylmethylsulfonyl fluoride, 0.5 mM sodium orthovanadate) for 30 min in ice. The lysates were then cleared by centrifugation (10 min at 15,000 rpm, 4 °C), and protein concentration was determined using the Bradford method [47]. Equal amounts of protein (20 μg) were resolved by electrophoresis by 10% SDS-polyacrylamide gel electrophoresis and transferred to nitrocellulose membranes. Blots on membranes were washed with TBST (10 mM Tris–HCl [pH 7.6], 150 mM NaCl, 0.05% Tween-20), blocked with 5% skim milk for 1 h, and incubated with the appropriate primary antibody. Membranes were then washed, and primary antibodies were detected with goat anti-rabbit IgG or goat anti-mouse IgG conjugated to horseradish peroxidase. The bands were then visualized by enhanced chemiluminescence (Amersham Pharmacia Biotech).

2.12. Immunoprecipitation and kinase assays

Cells were extracted for 30 min in ice-cold lysis buffer (0.1 mM dithiothreitol, 8 mM β-glycerophosphate, 1 mM ethylenediaminetetraacetic acid, 150 mM sodium chloride, 50 mM sodium fluoride, 0.5% Nonidet P-40, 50 mM Tris–HCl (pH 7.4), 1 μg/ml aprotinin, 100 mM phenylmethylsulphonyl fluoride (PMSF), 10 μg/ml soybean trypsin inhibitor, 10 μg/ml tosylphenylalanine chloromethane, 1 μg/ml leupeptin), and further processed as described previously [13,22]. Briefly, extracts were cleared by centrifugation at 15,000 × *g* for 5 min at 4 °C and stored at −80 °C until use. After thawing, protein concentration was determined using a DC protein assay kit (Bio-Rad). Extracts were incubated with the appropriate antibodies for 1 h in ice. Immunoprecipitates were collected on Protein G agarose beads by overnight rotation, washed four times with lysis buffer, re-suspended in 2× Laemmli sample buffer, and subjected to SDS-PAGE followed by Western blot analysis. To control for the specificity of the immunoprecipitation reaction, a control sample containing only cell lysate and G protein-coupled beads, but no antibody, was included in each set of immunoprecipitated samples (no antibody control). For kinase assays, immunoprecipitates were prepared as above, except that the last two washes were performed using kinase assay buffer (50 mm *N*-(2-hydroxyethyl) piperazine-*N*′-(2-ethanesulfonic) acid (HEPES), pH 7.5; 8 mM β-glycerophosphate; 1 mM dithiothreitol; 10 mM $MnCl_2$; 10 mM $MgCl_2$). For CDK2, kinase reactions were carried out for 30 min at 37 °C in a total volume of 25 μl in kinase assay buffer supplemented with 100 μg/ml histone H1 (type III-S) and 40 μCi/ml [^{32}P]ATP. For CDK4, kinase reactions were carried out for 30 min at 30 °C in a total volume of 25 μl in kinase assay buffer supplemented with 160 μg/ml

GST-pRb (type III-S) and 40 μCi/ml [^{32}P]ATP. For the negative control, samples of kinase reactions no antibody control and substrate control were used. Reactions were terminated by addition of 2× Laemmli sample buffer. Each reaction mix was then subjected to SDS-PAGE. Autoradiographies of gels and bands were quantified on a Molecular Dynamics PhosphorImager plate.

2.13. Statistical analysis

Data are presented as means ± S.E.M. of five or more independent experiments, each with two replicates. Statistical significance was determined by Student's *t*-test or one-way ANOVA plus a *post-hoc* Tukey's test. Values of $p<0.05$ were considered as statistically significant.

3. Results

3.1. Spontaneous Ca^{2+} oscillations are restricted to the G_1/S phase transition during neuronal differentiation of CSCs and MSCs

To study neuronal differentiation in embryonic (CSCs) and somatic (MSCs) stem cell lines and the role of calcium events in this process, we monitored the occurrence of calcium oscillations in undifferentiated cells and differentiated neural progenitor cells (NPCs). Spontaneous Ca^{2+} oscillations were present in 37% and 64% of undifferentiated CSCs and MSCs, respectively. During neuronal differentiation, the number of oscillating cells did not change. However, there were significant differences in amplitude, as NPCs had higher amplitude calcium events than undifferentiated cells (Supplementary Fig. 1). To determine if these spontaneous Ca^{2+} events vary throughout the cell cycle, we synchronized cells at distinct phases of the cell cycle and analyzed their Ca^{2+} oscillations. Cell cycle distributions were obtained by analyzing histograms of cells stained with propidium iodide and separated through fluorescence-activated cell sorting (FACS).

Undifferentiated cells were synchronized at the G_1/S transition with mimosine (MIM, 500 μM), an iron chelator that inhibits DNA replication in mammalian cells [41,48]. To study cells in the G_2/M transition, cells were incubated with demecolcine (DC, 20 ng/ml), a substance that depolymerizes microtubules, blocking mitosis at metaphase. FACS analysis of PI-stained MIM- and DC-treated cultures revealed a shift of the cell cycle distribution from control conditions. In CSC and MSC MIM-treated cultures, the majority of cells were in G_1, in both NPCs and undifferentiated cells, whereas in DC-treated cultures, cells accumulated in the G_2/M transition (Fig. 1). This demonstrates that we successfully arrested the cell cycle in the G_1/S and in the G_2/M transitions, respectively, with MIM and DC (Fig. 1), as shown previously [13,17,22,49–51].

The number of cells with spontaneous Ca^{2+} oscillations after treatment with MIM increased in both undifferentiated cells and NPCs from CSCs and MSCs (Table 2). Moreover, these increases were correlated with the total number of cells synchronized in the G_1 phase of the cell cycle (Fig. 1). In undifferentiated cells and NPCs treated with DC, only a low percentage of cells within individual colonies had spontaneous Ca^{2+} oscillations. Interestingly, the number of cells with such oscillations correlated with the number of cells in G_1 (Fig. 1). We also used other cell cycle inhibitors (HU and NOC) to verify if the shift in the total number of cells presenting spontaneous Ca^{2+} oscillations was due to a reaction to DC and MIM that is unrelated to control of the cell cycle (Fig. 1).

To synchronize cells in the G_1/S transition, we used 2 mM hydroxyurea (HU), a drug that arrests cells in the S phase by blocking deoxynucleotides synthesis [42]. In order to arrest the cells in the transition from G_2 to M, cells were incubated with NOC (100 ng/ml), a drug that disrupts mitotic spindles [44,48]. Treatment with HU and NOC induced effects that were similar to exposure to MIM and DC, respectively (Fig. 1). Thus, different drugs that arrest the cell cycle in the same transition points produced similar results. This strongly suggests that the observed increase in the fraction of G_1 cells displaying calcium oscillations is indeed due to arrest in the G_1/S transition. Importantly, the frequency and amplitude of Ca^{2+} oscillations did not differ between control and G_1/S synchronized cells (Supplementary Fig. 1).

These results show that cells displaying calcium oscillations are primarily in G_1/S. Moreover, these data indicate that while the fraction of cells displaying calcium oscillations is modulated throughout the cell cycle, the frequency and amplitude of these events are not. Strikingly, the same results were found in NPCs and undifferentiated cells derived from two different lineages, suggesting that this event may be conserved across lineages.

3.2. Maintenance of Ca^{2+} oscillations

Intracellular Ca^{2+} concentration ($[Ca^{2+}]_i$) is controlled by multiple mechanisms that regulate Ca^{2+} influx from internal and external sources. Increases in intracellular Ca^{2+} due to release from the endoplasmic reticulum (ER) is controlled by RyRs [35] and IP_3Rs [50]. This activity is counter-balanced by Ca^{2+} pumps, such as the Sarco/Endoplasmic Reticulum Ca^{2+}-ATPase (SERCA) [51]. Calcium influx from external sources can be mediated by voltage-gated calcium channels and store-operated calcium channels (SOCs) [52,53]. We studied the influence of calcium influx from both external and internal sources in the spontaneous Ca^{2+} oscillations observed in the G_1/S transition.

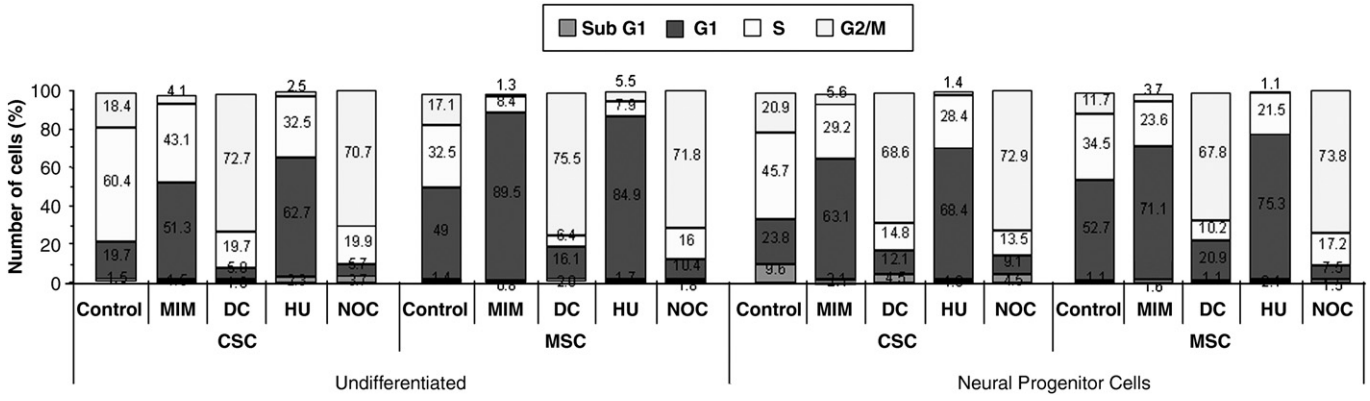

Fig. 1. Pharmacologically induced changes of cell cycle distribution in undifferentiated and neural progenitor cells of carcinoma stem cells (CSC) and mesenchymal stem cells (MSC). Bar graph shows the cell cycle distribution of three independent experiments analyzed using fluorescence-activated cell sorting (FACS). The graph allows the direct comparison of the percentage of cells that reside in the G_0/G_1, S, or G_2/M phases of the cell cycle in control conditions and after treatment with mimosine (MIM, 500 μM), demecolcine (DC, 20 ng/ml), nocodazole (NOC, 100 ng/ml) or hydroxyurea (HU, 2 mM). Data are presented as means from three independent experiments.

Table 2
Percentage of oscillating cells in control and after mimosine (MIM, arrests cells in G_1 phase), demecolcine (DC, arrests cells in metaphase), hydroxyurea (HU, synchronize cells in S-phase), or nocodazole (NOC, arrest the cell cycle at G_2/M phase) treatment, respectively, for neuronal progenitor cells from carcinoma (CSC) and mesenchymal (MSC) stem cells.

% of oscillating cells	Undifferentiated		Neural progenitor cells	
	CSC	MSC	CSC	MSC
Control	23.1 ± 6.2	53.8 ± 8.3	30.6 ± 6.8	56.1 ± 5.4
MIM	60.8 ± 12.5**	92.1 ± 11.6*	71.4 ± 10.3**	75.8 ± 8.2*
HU	65.7 ± 10.7**	89.6 ± 9.2*	67.6 ± 8.5*	69.8 ± 7.5
DC	9.6 ± 8.2*	13.4 ± 9.1**	12.5 ± 9.8**	17.2 ± 5.9**
NOC	6.2 ± 4.4*	8.6 ± 7.4**	5.9 ± 4.2**	8.0 ± 7.9**

Mimosine (MIM; 500 μM); demecolcine (DC; 20 ng/ml); nocodazole (NOC; 100 ng/ml), and hydroxyurea (HU; 2 mM). Data presented are means ± S.E.M. *$p<0.05$, **$p<0.001$ relative to control conditions.

The influence of internal calcium stores on calcium transients was evaluated by treating cells with the SERCA inhibitor cyclopiazonic acid (CPA). CPA depletes intracellular calcium stores, thus abolishing the contribution of these stores to the observed oscillations. Interestingly, calcium oscillations were undetectable in undifferentiated cells exposed to CPA. However, in NPCs CPA had a less drastic effect, only reducing the amplitude and frequency of the oscillations (Fig. 2 and Supplementary Fig. 2). This result suggests that internal calcium stores are required to produce these calcium events in undifferentiated cells, while NPCs can maintain them through other mechanisms, such as by activation of voltage gated calcium channels [10,21,54]. To evaluate if extracellular Ca^{2+} stores participate in spontaneous Ca^{2+} oscillations in undifferentiated cells and NPCs we exposed cells in the presence and absence of MIM to a Ca^{2+}-free extracellular solution, which was obtained by adding the calcium chelator EGTA. Interestingly, the amplitude and frequency of Ca^{2+} oscillations were reduced, but less robustly than in CPA-treated cells (Fig. 2 and Supplementary Fig. 2). These results show that while external calcium may influence the amplitude and frequency of these oscillations, presumably because they may be necessary to replenish intracellular stores.

To characterize the contribution of external calcium stores we sought to identify which channels mediate the influx of external calcium necessary to maintain Ca^{2+} oscillations. To this end, cells were exposed to the SOC inhibitor lanthanum (50 μM), and the L-type Ca^{2+} channel inhibitor, nifedipine (5 μM). Interestingly, inhibition of L-type calcium channels and SOCs abolished calcium events in undifferentiated cells and NPCs (Fig. 3 and Supplementary Fig. 3). It is noteworthy that these results were conducted in the presence of thapsigargin, a drug that inhibits the ER SERCA pump, abolishing the contribution of internal stores to the

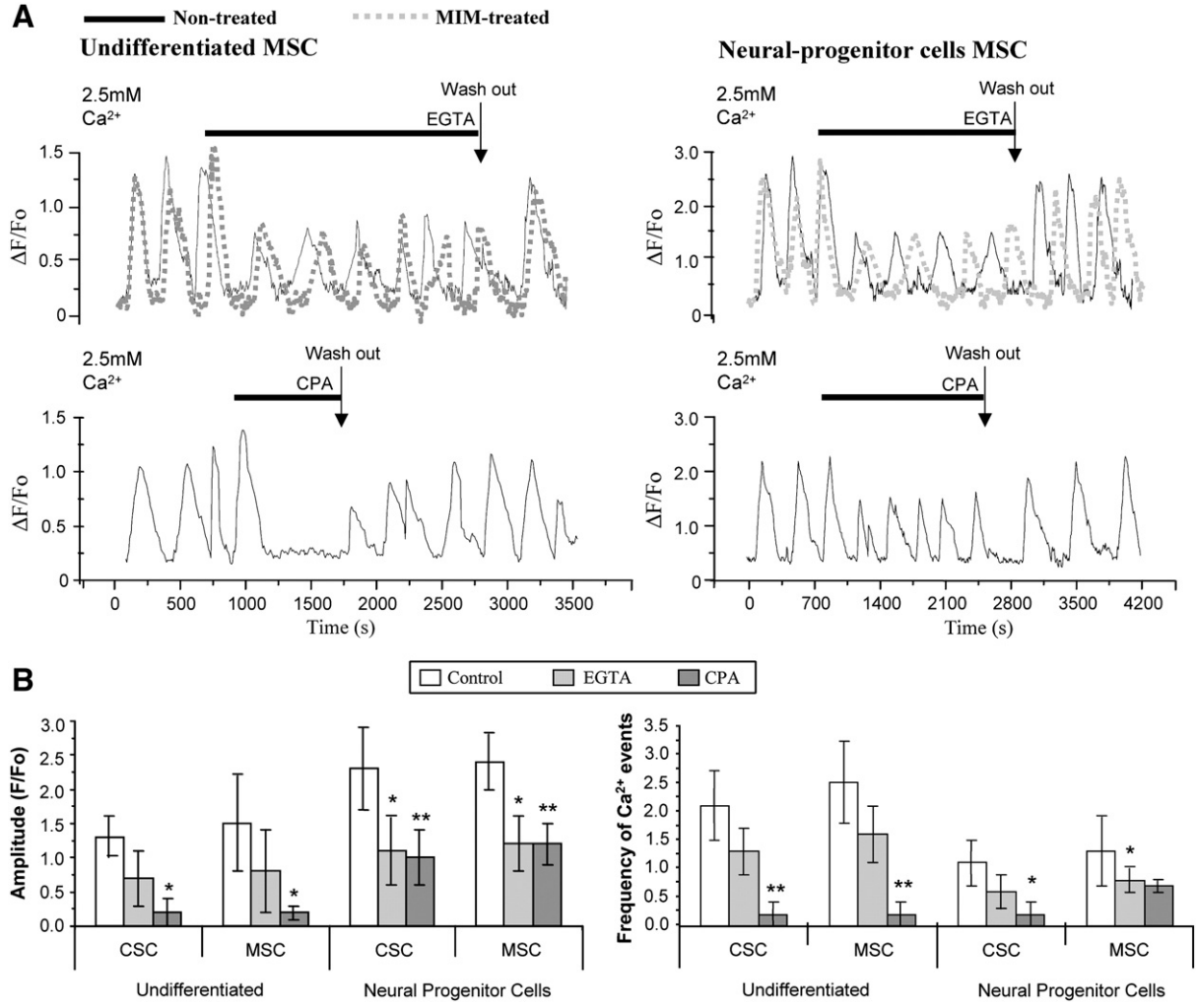

Fig. 2. Characterization of spontaneous Ca^{2+} oscillations in undifferentiated and neural progenitor cells derived from MSCs. (A) Representative traces showing calcium oscillations in control cultures (black traces) and mimosine-treated (MIM, 500 μM) cells (dashed gray traces). Note that the SERCA inhibitor cyclopiazonic acid (CPA, 100 μM) abolishes calcium transients in undifferentiated cells, but only decreases their amplitude in NPCs. Similar observations were obtained in four different experiments for each line cell. (B) Bar graphs showing average changes in amplitude (left panel) and frequency (right panel) of calcium oscillations in cells treated with EGTA and CPA. The total number of cells analyzed in each experiment was 20–26.

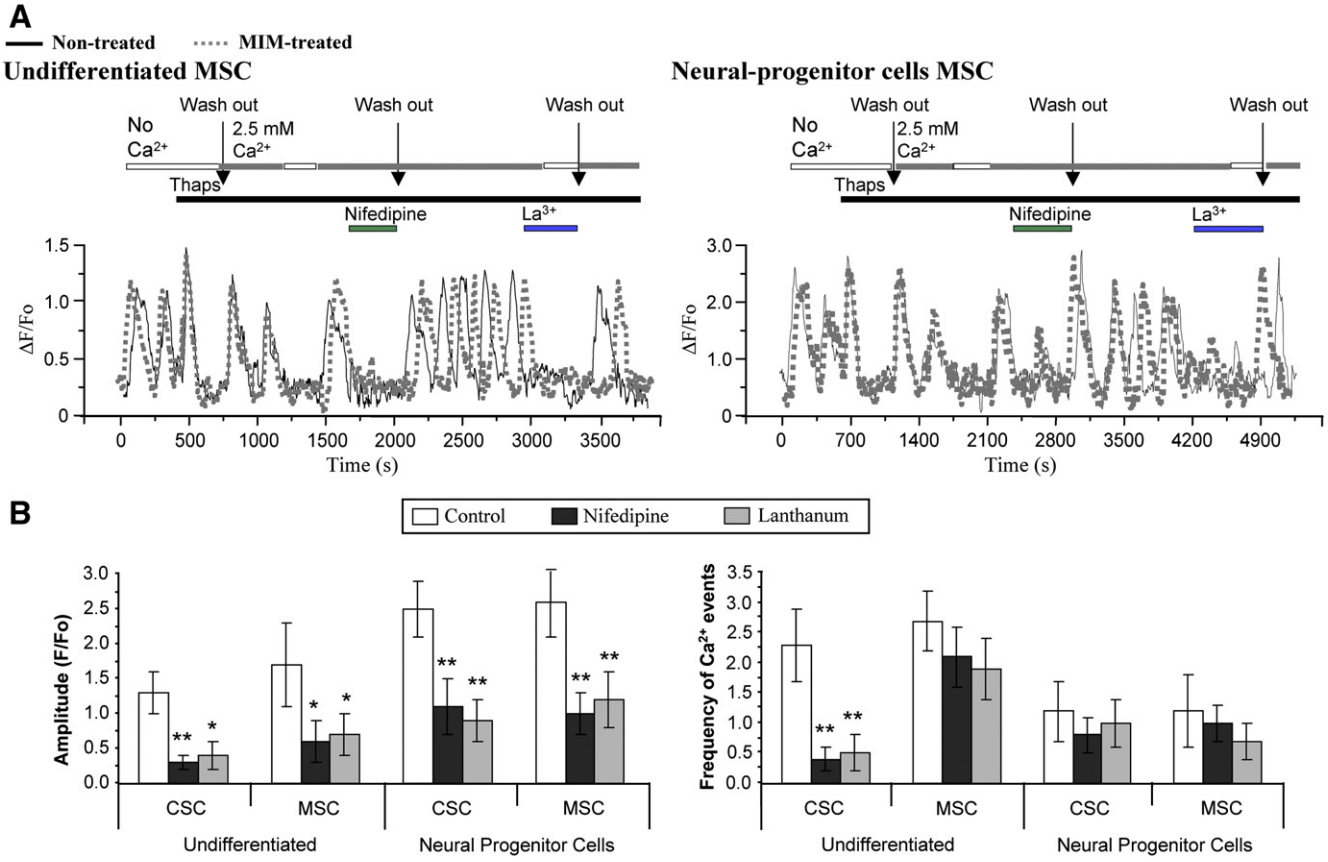

Fig. 3. Involvement of L-type calcium channels and through store-operated Ca^{2+} (SOC) channels in spontaneous Ca^{2+} oscillations. (A) Ca^{2+} measurements in a single undifferentiated (Und) or neural progenitor cells (NPC) from mesenchymal stem cells (MSC), respectively, in non-treated (black traces) and mimosine (MIM; 500 μM) treated cultures (dashed gray traces). Changes in $[Ca^{2+}]_i$ during store depletion with the endoplasmic reticulum Ca^{2+}-ATPase inhibitor thapsigargin (Thaps, 1 μM) in the absence (1 mM EGTA) and presence of $[Ca^{2+}]_o$ (2.5 mM Ca^{2+}) and during superfusion with the SOC inhibitor lanthanum (La^{3+}, 50 μM), and the L-type Ca^{2+} channel inhibitor, nifedipine (5 μM). Inhibition of L-type calcium channels and SOCs abolished calcium events in undifferentiated cells and NPCs. La^{3+} reversibly blocked about 81% of the Ca^{2+}-entry induced by depletion of the intracellular Ca^{2+} stores. (B) Bar graphs showing average changes in amplitude (left panel) and frequency (right panel) of calcium oscillations in cells treated with nifedipine and La^{3+}. Data are presented as means ± (SD). $n = 38–47$ cells for each experiment.

oscillations. This allows to isolate the effects of extracellular calcium influx. These data show that L-type channels and SOCs are involved in the generation of calcium events in undifferentiated cells and in NPCs.

We next investigated whether replenishment of internal Ca^{2+} stores through SOCs contribute to Ca^{2+} oscillations. Previous data have shown that SOCs are present in mesenchymal and embryonic stem cells [10,11], raising the possibility that these channels may contribute to the calcium oscillations observed here. To determine if SOCs contribute to the replenishment of intracellular Ca^{2+} stores we exposed cells to a Ca^{2+}-free solution in the presence of thapsigargin, a Ca^{2+}-ATPase (SERCA) inhibitor. Thapsigargin induced a transient increase in internal Ca^{2+} due to the uncompensated release of Ca^{2+} from intracellular stores. As depletion of intracellular stores triggers calcium influx through SOCs, it is likely that the observed increase in calcium oscillations following the addition of Ca^{2+} (2.5 mM) is due to SOC opening (Fig. 3 and Supplementary Fig. 3). This result indicates that replenishment of intracellular Ca^{2+} stores in CSC and MSC cells is mediated by influx of extracellular Ca^{2+} through SOCs. However, extracellular Ca^{2+} is not required for the induction of Ca^{2+} oscillations, as they are still observed in the absence of extracellular calcium (see the first 500 s of the traces shown in Fig. 3A).

3.3. Spontaneous Ca^{2+} oscillations are regulated by IP_3Rs in undifferentiated cells and by IP_3Rs and RyRs in neural progenitor cells

We also analyzed the contribution of internal calcium stores to calcium oscillations. RyR mRNA was observed after, but not before induction of neuronal differentiation (Supplementary Fig. 6), as previously described [13,55]. The ER channel IP_3R, on the other hand, was present during all developmental stages of stem cells (Supplementary Fig. 6) [13,55]. To determine which channels mediate spontaneous Ca^{2+} oscillations in undifferentiated stem cells and NPCs we exposed cell cultures to the IP_3R antagonist 2-APB (10 μM), or to ryanodine (10 μM), which in this concentration acts as a RyR antagonist [33]. Calcium transients were abolished in undifferentiated cells treated with IP_3R inhibitors, such as 2-APB, U-73122 or xestopongin C (Fig. 4 and Supplementary Fig. 4). On the other hand, exposure to the RyR inhibitor ryanodine (10 μM) in undifferentiated cells did not block spontaneous Ca^{2+} oscillations and no difference in oscillation frequency or amplitude was found (Fig. 4 and Supplementary Fig. 4). To confirm the result, we treated undifferentiated cells with the RyR agonist and IP_3R inhibitor caffeine (10 mM). Undifferentiated cells treated with caffeine did not display calcium oscillations as previously demonstrated (Fig. 4 and Supplementary Fig. 4) [13,55].

Conversely, in NPCs, caffeine (10 mM) caused a transient peak in calcium (Fig. 4 and Supplementary Fig. 4) that is attributable to a caffeine-induced release from ryanodine-sensitive stores, indicating the involvement of RyRs in calcium oscillations in NPCs. The subsequent depression of $[Ca^{2+}]_i$ can be either due to suppression IP_3Rs [56–59] or to depletion of ryanodine-sensitive calcium stores [59,60].

Consistent with a role for RyRs in calcium events in NPCs, treatment with ryanodine (10 μM) reduced the amplitude and frequency of Ca^{2+} oscillations (Fig. 4 and Supplementary Fig. 4). Unlike in undifferentiated cells, oscillations in NPCs were reduced, but not abolished by the IP_3R

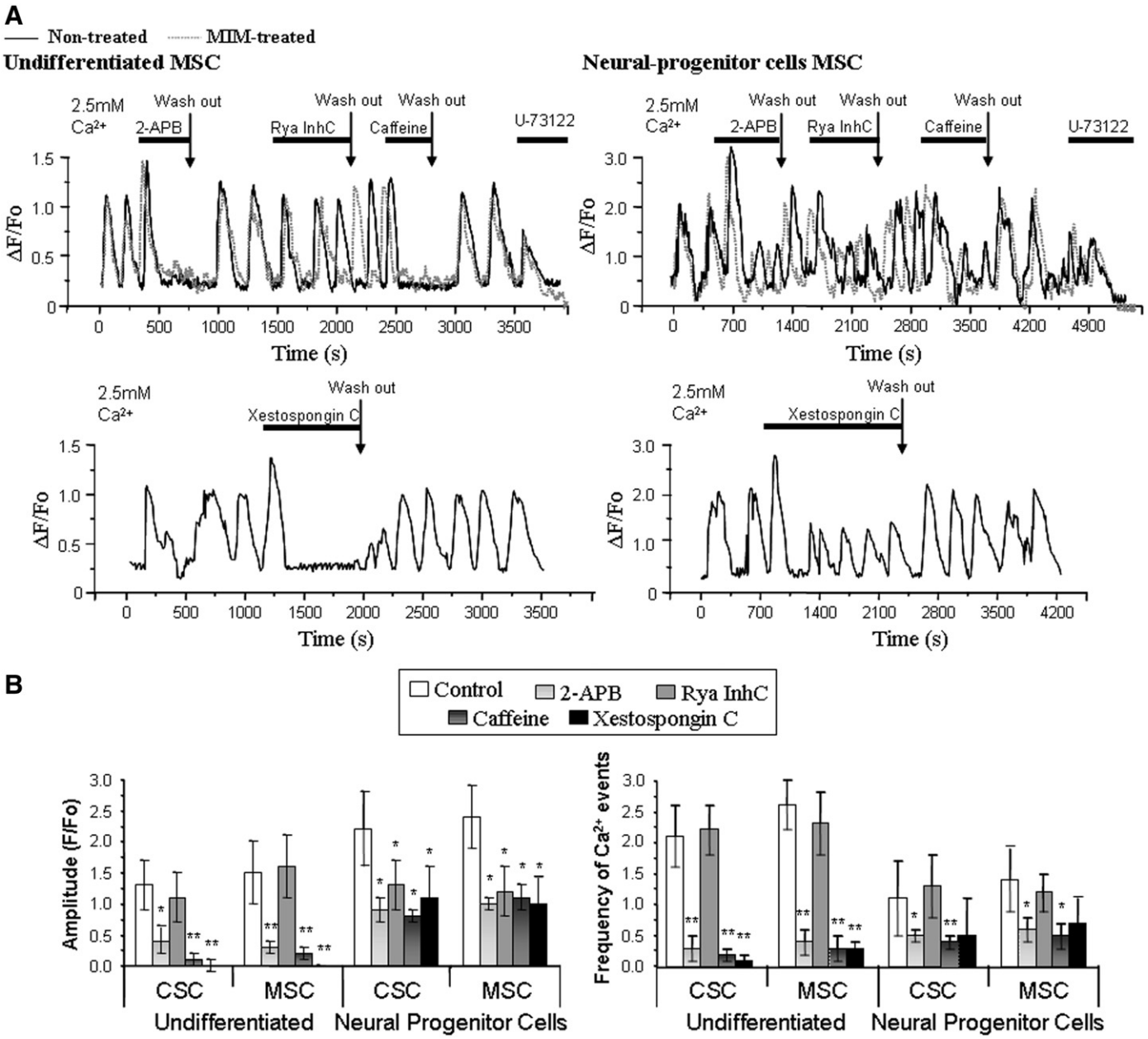

Fig. 4. Spontaneous Ca^{2+} oscillations require inositol 1,4,5-trisphosphate receptor (IP_3R)-mediated Ca^{2+} release. (A) Upper panels: Representative recordings of $[Ca^{2+}]_i$ within a single cell during superfusion with the IP_3R antagonist 2-aminoethoxydiphenyl borate (2-APB, 10 μM), or with Ryanodine (Rya InhC, 10 μM), which at this concentration acts as a RyR antagonist. Cells were also treated with caffeine (10 mM), which in this concentration inhibits IP_3Rs and activates ryanodine receptors. Cells were also exposed to the phospholipase C (PLC) inhibitor U-73122 (5 μM). IP_3R-mediated Ca^{2+} oscillations in non-treated and mimosine (MIM; 500 μM) treated cultures from undifferentiated and neural progenitor cells (NPC) of mesenchymal stem cells (MSC), respectively. Lower panels: Representative recordings of $[Ca^{2+}]_i$ showing the effect of xestospongin-C in calcium oscillations of undifferentiated (left) and NPCs (right) derived from MSCs. The total number of cells analyzed in each experiment was 45–58. (A, lower panels) Representative recordings of $[Ca^{2+}]_i$ within a single cell during superfusion with the IP_3R antagonist xestospongin C, which abolished spontaneous oscillations of $[Ca^{2+}]_i$ in undifferentiated and decreased their amplitude in neural progenitor cells from MSCs. (B) Bar graphs showing average changes in amplitude (left panel) and frequency (right panel) of calcium oscillations in cells treated with the drugs shown in (A). Data are presented as means ± (SD).

inhibitor xestopongin C. This suggests that NPCs can maintain calcium oscillations through mechanisms independent of IP_3R signaling, such as RyR-mediated Ca^{2+} release [13,21,54,61].

Thus, the finding that Ca^{2+} transients were abolished in undifferentiated cells in the presence of caffeine suggests that IP_3Rs, but not RyRs, are required for maintaining these oscillations. Application of 2-APB resulted in a reversible inhibition of Ca^{2+} oscillations, indicating a contribution from IP_3-sensitive stores and SOCs (Fig. 4 and Supplementary Fig. 4). The same results were found when cells were treated with U-73122, a drug that decreases IP_3R signaling by inhibiting PLC-mediated production of IP_3. Cells were also treated with the membrane-permeable inhibitor of IP_3Rs, Xestospongin C (XeC). Cells were treated with U-73122 and XeC because the effect observed with 2-APB could be due to its effect on gap junctions and SOCs [62–64]. Spontaneous oscillations were also decreased by U-73122, XeC and caffeine in both undifferentiated and NPCs from CSC and MSC cells. Our data consistently indicate that in both CSCs and MSCs, spontaneous oscillations in undifferentiated cells depend on the release of Ca^{2+} from IP_3R-regulated intracellular stores, while in NPCs, both RyRs and IP_3Rs contribute to these oscillations (Fig. 4 and Supplementary Fig. 4).

3.4. Role of spontaneous Ca^{2+} events in cell cycle progression and cell proliferation

It has been reported that cell cycle progression occurs synchronously with spontaneous Ca^{2+} events [17,65,66]. These events can be

induced by IP_3 in cells in culture and in early embryos [4,67]. We further studied the role of intracellular calcium dynamics in this process in undifferentiated cells and NPCs, derived from CSCs and MSCs. To this end, we determined the proliferation rate of cells treated with the PLC-β blocker U-73122 (5 μM) and the intracellular Ca^{2+} chelator BAPTA-AM (10 μM). Treatment with these drugs significantly decreased rates of proliferation (Fig. 5 and Table 3). Importantly, U-73343, a structural analog of U-73122 that does not inhibit PLC-β activity, did not affect growth rates (Fig. 5A, B). Cells were also treated with 2-APB (10 μM), xestospongin C (XeC, 1 μM), and thapsigargin (1 μM) to evaluate the growth rate of undifferentiated CSCs and MSCs. Blocking calcium oscillations by decreasing IP_3R activation with XeC and 2-APB induced a significant slowing in cell cycle progression (Fig. 5A, B). Additional studies were carried out to elucidate if promotion of calcium oscillations through activation of IP_3Rs affect the rate of proliferation in CSCs and MSCs. Cells were treated with either AdA (2 nM), an IP_3R agonist, or thimerosal (10 μM), a thiol reagent described to increase the sensitivity of IP_3R for its agonist. Both induced an increase in the rate of proliferation of undifferentiated CSCs and MSCs (Fig. 5A, B). These results suggest the involvement of PLC-β and IP_3-induced release of Ca^{2+} from internal stores in signaling pathways leading to proliferation. Similar results were obtained with BrdU incorporation assays (Fig. 5C), showing that the results in Fig. 5A and B are due to increased proliferation, and not thus cannot be attributed to a decrease in cell death.

Table 3
Cell cycle progression of undifferentiated carcinoma (CSC) and mesenchymal stem cells (MSC) cultures.

Growth rate (in hours)	Undifferentiated	
	CSC	MSC
Control	18.1 ± 0.5	28.8 ± 1.0
U-73343	18.7 ± 1.4	28.6 ± 0.7
U-73122	23.0 ± 1.3*	36.9 ± 1.7*
BAPTA-AM	27.1 ± 2.1**	42.8 ± 2.7**
Thapsigargin	26.4 ± 1.1**	40.5 ± 2.3**
2-APB	22.0 ± 1.2*	38.2 ± 1.8**
Xestopongin C	21.7 ± 1.5*	39.5 ± 1.2**
Nifedipine	20.1 ± 2.1*	33.6 ± 1.3*
Lanthanum	19.5 ± 1.8*	33.4 ± 2.3*
AdA	13.3 ± 0.1**	22.2 ± 0.7**
Thimerosal	14.0 ± 0.1**	21.1 ± 0.6**

U-73343 (5 μM), U-73122 (5 μM), BAPTA-AM (10 μM), thapsigargin (1 μM), 2-aminoethoxydiphenyl borate (2-APB, 10 μM), Xestopongin C (10 μM), nifedipine (5 μM), lanthanum (100 μM), adenophostin-A (AdA, 2 nM), thimerosal (10 μM). Data presented are means ± S.E.M. *$p<0.05$, **$p<0.001$ relative to control conditions.

Strikingly, exposure to drugs that decrease calcium oscillations, such as U-73122, 2-APB, lanthanum, nifedipine or BAPTA-AM decreased the number of cells in G_2/M but increased the number of cells in the G_1 and S phases, both in undifferentiated cells and NPCs (Fig. 6). Conversely, exposure to the RyR agonist ryanodine (1 μM), or

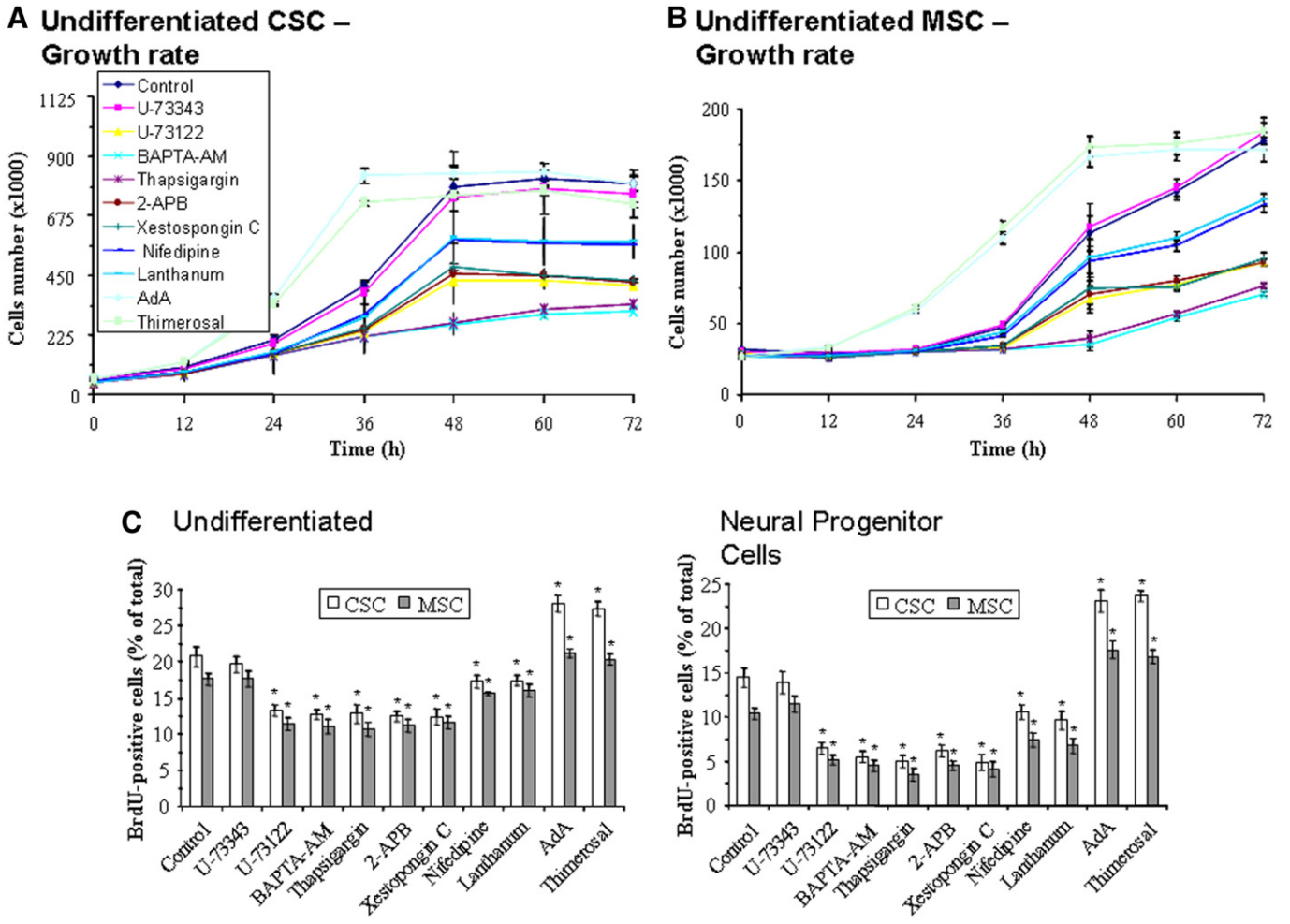

Fig. 5. IP_3R activation increases cell proliferation. Curves show proliferation of CSCs (A) and MSCs (B) treated with 5 μM U-73343, 5 μM U-73122, 10 μM BAPTA-AM, 1 μM thapsigargin, 10 μM 2-aminoethoxydiphenyl borate (2-APB), 1 μM Xestospongin C, 5 μM nifedipine, 50 μM lanthanum, 2 nM adenophostin-A (AdA) or 10 μM thimerosal. (C) Bar graphs showing % of BrdU-positive cells in cultures exposed to the same drugs used in (A), for undifferentiated cells (left panel) and NPCs (right panel). Data are presented as normalized changes from control cultures, and are presented as mean values ± S.E.M.; *$p<0.001$ compared with control data. Significance of the change in cell cycle distribution was confirmed using the chi-square test: $p<0.005$. $n=4$–6 for each drug treatment.

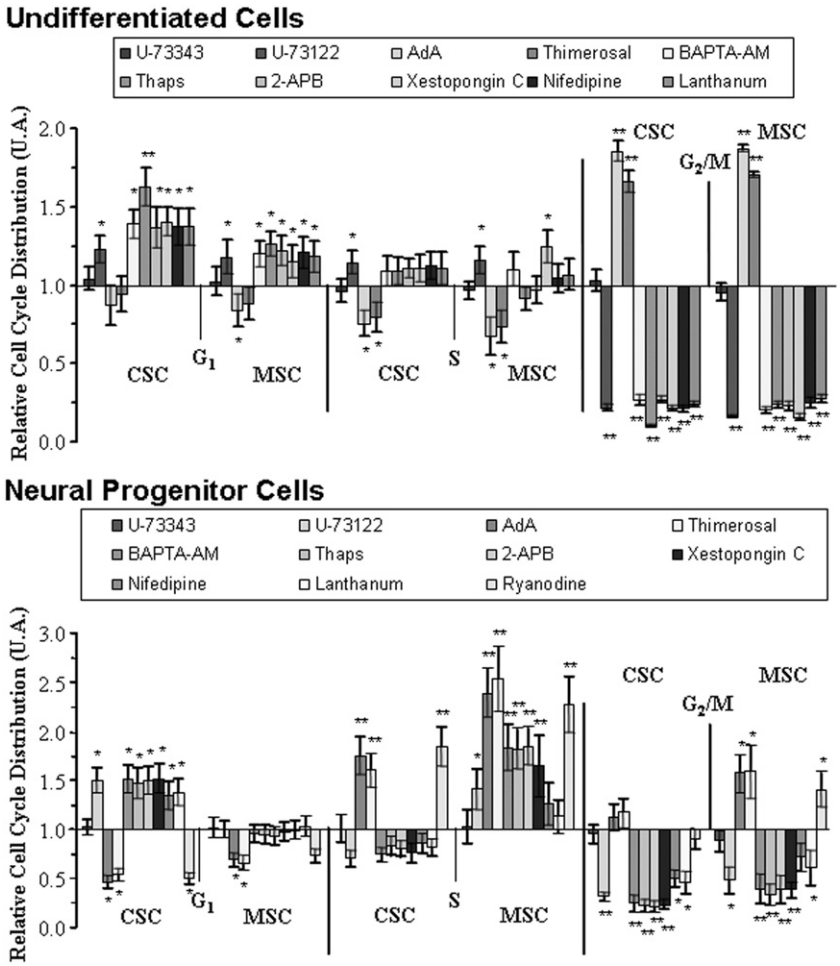

Fig. 6. IP_3R activation shifts the cell cycle distribution toward the G_2/M transition phase of the cell cycle. Undifferentiated cells and NPCs were treated with 5 μM U-73343, 5 μM U-73122, 10 μM BAPTA-AM, 1 μM thapsigargin, 10 μM 2-aminoethoxydiphenyl borate (2-APB), 1 μM Xestospongin C, 5 μM nifedipine, 50 μM lanthanum ($n=3$), 2 nM adenophostin-A (AdA), 10 μM thimerosal compared to the control cells. NPC cultures were also treated with ryanodine 1 μM. Data are presented as normalized changes from control cultures. Data are presented as mean values ± S.E.M.; $^*p<0.05$, $^{**}p<0.001$ compared with control data. Significance of the change in cell cycle distribution was confirmed using the chi-square test: $P<0.005$). $n=3$–5 for each drug treatment.

to the IP_3R agonists AdA and thimerosal increased the fraction of cells in G_2/M (Fig. 6). To characterize the participation of extracellular Ca^{2+} stores on cell cycle progression we used nifedipine, an L-type calcium channel blocker, and lanthanum, a SOC inhibitor. Both nifedipine and lanthanum induced a significant increase on cell turnover time (Fig. 5 and Table 3).

These data indicate that PLC-mediated Ca^{2+} oscillations may play an important role in cell cycle progression through the G_1/S phase in undifferentiated CSC and MSC cells.

3.5. Involvement of IP_3R-induced signaling in cyclin expression

We showed that decreasing calcium oscillations by blocking IP_3R responses reduced the number of cells residing in G_2/M and the rate of proliferation of undifferentiated cells and NPCs (Fig. 5C). This result suggests that the expression of cell cycle regulators, such as cyclin D1 may be affected by altered IP_3R signaling. To further study this issue we studied the effects of treating cells with the purinergic receptor agonist ATP, as ATP induces calcium transients mediated by IP_3R activation [20,49]. ATP was found to increase levels of proteins that are highly expressed in proliferating cells, such as cyclin D1, cyclin E, CDK2, and CDK4 (Fig. 7 and Supplementary Fig. 5). Conversely, the opposite effect was found when cells were exposed to drugs that suppress calcium waves, such as the IP_3R pathway inhibitors 2-APB, xestospongin C, wortmanin, and PD 98059 (Fig. 7 and Supplementary Fig. 5). These results were observed with undifferentiated cells and NPCs derived from both CSCs and MSCs. To verify if IP_3R was indeed the calcium channel that mediated the effects observed on progression of the cell cycle, we treated NPCs with antagonists of other calcium channels, such as thapsigargin, lanthanum, and ryanodine at inhibitory concentrations (10 μM) in the presence or absence of ATP, and evaluated their effect on cyclin expression. Treatment with thapsigargin alone and in the presence of ATP, decreased and maintained similar to the control, respectively, protein levels of cyclin D1, cyclin E, CDK2, and CDK4. Conversely, when NPCs were treated with lanthanum and ryanodine (10 μM) no effect on protein levels was observed. Although, when NPCs were treated with the same drugs in the presence of ATP protein levels presented a significant increase when compared to control conditions. Furthermore, when NPCs were treated with U-73122 alone, cell cycle protein levels were reduced beyond control levels (Fig. 7C), indicating that IP_3Rs were responsible for the observed effect on progression of the cell cycle (Fig. 6).

3.6. Cell cycle kinase activity during MSC neuronal differentiation

The eukaryotic cell cycle is regulated primarily by a family of serine/threonine protein kinases, consisting of regulatory cyclin subunits and catalytic cyclin-dependent kinase (Cdk) subunits (for review see [68,69]). In mammalian cells, complexes of Cdk4 and

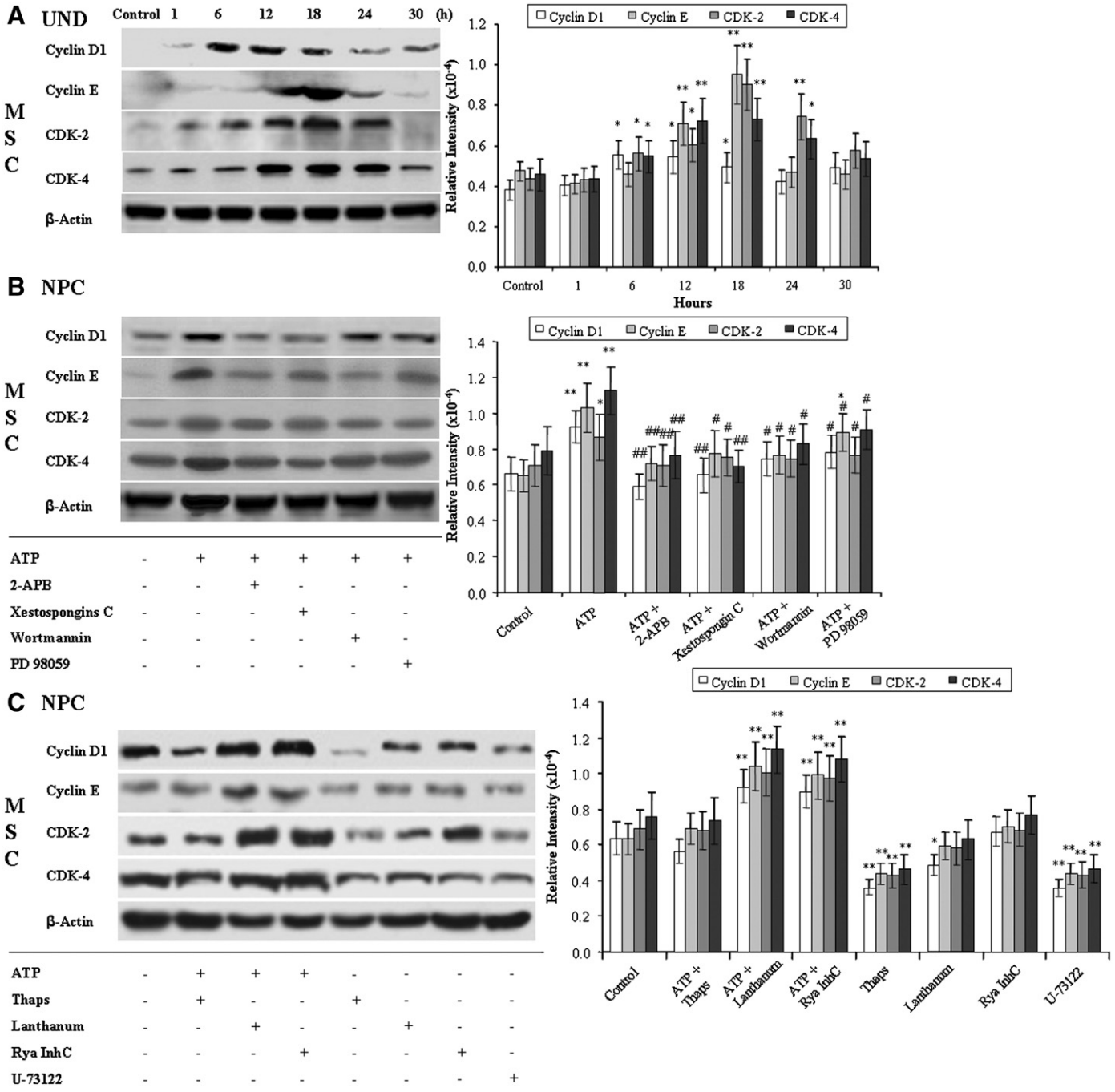

Fig. 7. Inhibition of IP_3Rs decreases protein levels of cell cycle regulators. Mesenchymal stem cells (MSC) were treated with adenophostin-A (2 nM, AdA) for periods between 1 and 30 h (A), or pretreated with 2-APB (10 μM), Xestospongin C (1 μM), wortmannin (1 μM), or PD 98059 (1 μM) for 30 min prior to incubating the cells with AdA (2 nM) for 3 h (B). Additional studies were performed on neural progenitor cells (NPCs). NPCs were treated for 30 min with ATP in the presence or absence of thapsigargin (Thaps, 1 μM), lanthanum (50 μM), ryanodine (10 μM), and U-73122 (5 μM) (C). The total lysates were then subjected to SDS-polyacrylamide gel electrophoresis and blotted with the cyclin D1, cyclin E, cyclin-dependent kinase 2 (CDK2), or CDK4 antibody. Each example shown (left panels) is representative of three experiments. Right panels (bar graphs) denote the mean ± S.E.M. of three experiments for each condition determined from densitometry relative to β-actin. *$p<0.05$ versus control; #$p<0.001$ versus AdA alone.

Cdk6 with D-type cyclins play a critical role in progression beyond the G_1 restriction point, while Cdk2/cyclin E complexes are required for the G_1 to S transition. Complexes of Cdk2-cyclin A function are involved in the progression of cells through S phase [70]. This process is negatively regulated by p27, as this protein binds to the cyclin E–Cdk2 complex, resulting in inhibition of its kinase activity [71,72]. If IP_3R-induced calcium oscillations promote proliferation, lower binding of cyclins E and A to p27 would be expected in cells treated with IP_3R agonists. In line with a role for calcium oscillations in proliferation, cells treated with the IP_3R agonist AdA had lower levels of Cyclin E and A bound to p27, as found through co-immunoprecipitation assays (Fig. 8). This result suggests that IP_3R signaling acts to increase proliferation by removing p27-mediated inhibition.

We also investigated the influence of IP_3R signaling on cell cycle regulatory proteins during neuronal differentiation. To this end, differentiating MSCs were treated with the IP_3R agonist AdA or with the IP_3R antagonist xestospongin C. Treatment with AdA increased levels of cyclins A and E, as found by both western blots and cyclin kinase activity (Fig. 7A and B). These results show that proliferation is

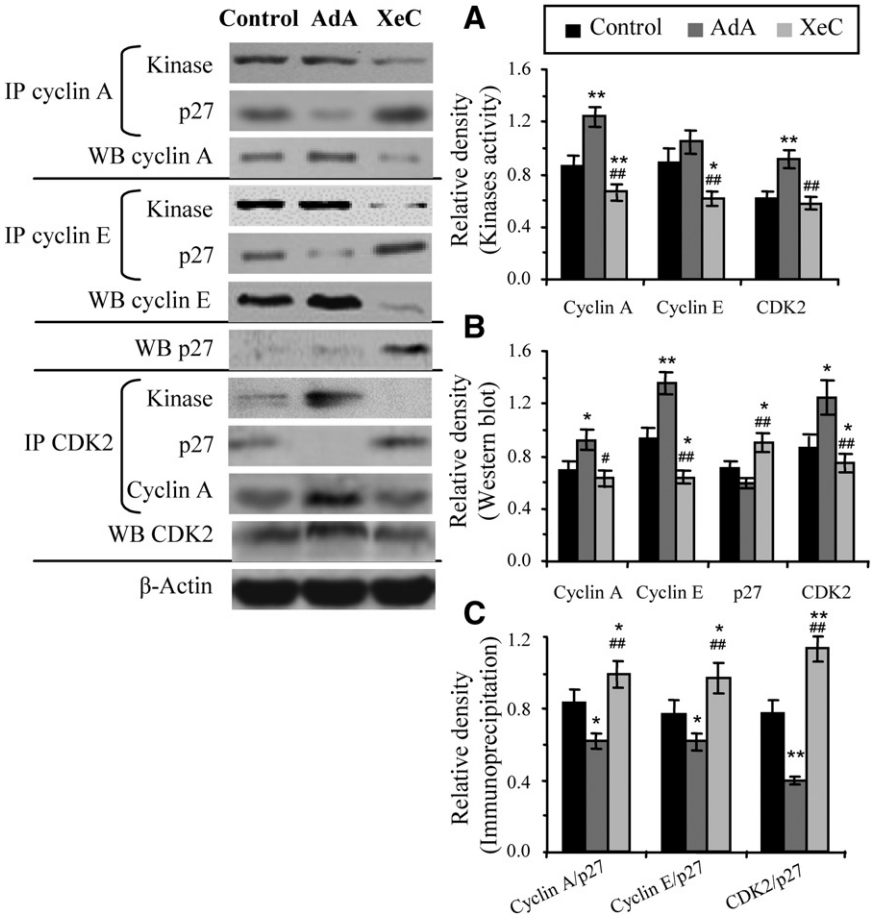

Fig. 8. IP_3R activation upregulates kinase activity of cyclins A and E and CDK2 and decreases their binding to the negative regulator p27 (A) Undifferentiated mesenchymal stem cells (MSCs), were treated with adenophostin A (AdA, 2 nM), an agonist for IP_3Rs, or Xestospongin C (XeC, 1 μM), a membrane permeable inhibitor of IP_3Rs). Cultures were lysed and used to immunoprecipitate cyclin A, cyclin E, CDK2 and p27. Kinase activity towards histone H1 in cyclin- and CDK2-immunoprecipitates was determined by autoradiography. Three independent replicates were quantified by densitometry. Graphs represent means ± SDs of autoradiographic signal normalized to control conditions. (B) Levels of p27 in cyclin A, cyclin E and CDK2 were determined by Western blotting, normalized to β-actin levels. Data are representative of three independent replicates. (C) Quantification of levels of complexes of p27 with cyclin A, cyclin E and CDK2 through immunoprecipitation in cultures treated with AdA and XeC. *$p<0.05$ versus control; **$p<0.001$ versus control; #$p<0.05$ versus AdA-treatment; #$p<0.001$ versus AdA-treatment.

decreased by drugs that block calcium oscillations by acting as IP_3R antagonists, while IP_3R agonists have the opposite effect. Furthermore, exposure to lanthanum and ryanodine (10 μM) do not change cyclin expression (Fig. 7C), consistent with the view that IP_3R, but not RyR activation modulates progression of the cell cycle. On the other hand, thapsigargin decreases cyclin expression (Fig. 7C). As thapsigargin depletes ER calcium stores, it is likely that the effect of thapsigargin on cyclin expression is mediated by disruption of IP_3R signaling.

4. Discussion

Cell cycle progression in stem cells and neural progenitor cells controls proliferation of neurons and glia during development of the central nervous system. Here we have demonstrated that in embryonic CSCs and adult MSCs cell cycle progression through the G_1/S transition is accompanied by spontaneous oscillations of $[Ca^{2+}]_i$. These Ca^{2+} oscillations are regulated by IP_3Rs and RyRs in NPCs, while in undifferentiated stem cells IP_3Rs, but not RyRs, appear to regulate these events. Our data also shows that inhibition of IP_3R pathways in undifferentiated cells impede progression of the cell cycle, possibly due to downregulation of cyclins A, D1 and E. Furthermore, activation of IP_3Rs increases cell proliferation. These data raise the possibility that control of calcium oscillations by IP_3Rs may play a role in cell cycle progression and cell proliferation.

4.1. Spontaneous Ca^{2+} oscillations in embryonic CSC and adult MSC

We have demonstrated that undifferentiated cells and NPCs from embryonic CSCs and adult MSCs display spontaneous Ca^{2+} oscillations (Fig. 2 and Supplementary Fig. 2), as in previous reports [13]. The present work shows that while the ER is the major source of Ca^{2+} for these oscillations, extracellular Ca^{2+} influx from SOCs is required to sustain these oscillations, presumably to refill intracellular stores of Ca^{2+}. Interestingly, these oscillations tend to occur at the G1/S transition, suggesting a role for calcium events in control of cell cycle progression.

ER intracellular Ca^{2+} stores are regulated by two families of receptors: IP_3Rs and RyRs [52,73]. Cytosolic IP_3 may be responsible for these Ca^{2+} oscillations (Fig. 4 and Supplementary Fig. 4), as suggested previously [13,74]. Interestingly, previous work has demonstrated that $[Ca^{2+}]_i$ changes can be induced by IP_3 oscillations through dynamic and rapid uncoupling of IP_3Rs [75], in line with our results. In both undifferentiated cells and NPCs, IP_3Rs regulate Ca^{2+} oscillations, whereas in later stages of differentiation both IP_3Rs and RyRs contributed to these events, consistent with previous work [13].

4.2. Involvement of IP_3R-induced Ca^{2+} oscillations in cell cycle progression

Some studies have demonstrated a role for IP_3 signaling pathways [78,79] and for IP_3-mediated Ca^{2+} release [17] in progression of the

cell cycle in embryonic stem cells. In line with these previous reports, our data show that in undifferentiated cells and NPCs from CSCs and MSCs proliferation was significantly decreased in the presence of drugs that prevent rises in $[Ca^{2+}]_i$ through PLC- and IP_3-mediated pathways (Figs. 5–8). These results are in good agreement with a recent report indicating that EGF stimulates proliferation of mouse embryonic stem cells via PLC-dependent changes in $[Ca^{2+}]_i$ [80]. Furthermore, we have previously shown that neurogenesis induced by cholinergic [21,22,81] and purinergic receptors [49] is mediated by IP_3Rs [13]. Thus, a role for IP_3R signaling in the maintenance of calcium oscillations is strongly supported by both by the current work and previous reports.

Interestingly, we found that expression levels of cell cycle regulatory proteins (cyclin D1, cyclin E, CDK2, and CDK4) were dependent on IP_3-mediated pathways. This suggests that IP_3 induces cell cycle progression beyond the G_1 phase of the cell cycle. These results also indicate that once IP_3Rs are activated, PKC transmits signals to the nucleus through one or more MAPK cascades and activates immediate early genes. Therefore, the present results show that IP_3 modulates proliferation, possibly due to its role in maintaining calcium oscillations. Moreover, as IP_3-induced calcium oscillations occur predominantly at the G1/S transition, these data are consistent with the hypothesis that calcium transients may be involved in cell cycle progression. However, it is important to consider that the effects observed on proliferation and progression of the cell cycle by IP_3R agonists and antagonists may be independent of calcium waves. For example, it is possible that activation of MAPK, phosphatidylinositol 3-kinase (PI3 kinase), and protein Kinase A pathway by IP_3R agonists [8,82,83] leads to increased proliferation. The finding that blocking calcium oscillations with RyR antagonists in NPCs also decrease proliferation [13] argues against this possibility. These oscillations may induce mitosis by activating calmodulin (CaM), which in turn may regulate the Ras/Raf/MEK/ERK pathway. CaM-binding proteins such as Ras-GRF and CaM-dependent protein kinase IV positively modulate ERK1/2 activation induced by either NGF or membrane depolarization [52,53,84]. These pathways play a role in initiating mitosis and are known to be activated by calcium oscillations [1,53,84].

However, data concerning the importance of these transients in cell cycle progression are contradictory. On one hand, data supporting a role for IP_3-mediated calcium oscillations in progression of the cell cycle are abundant. It has been shown that mitosis can be initiated by IP_3R-induced calcium transients in mouse embryos [85], sea urchin embryos [86], and in CSC and MSCs (Fig. 6). Moreover, in the sea urchin embryo a microinjection of calcium or IP_3 can induce entry into mitosis [86,87]. Conversely, microinjection of calcium chelators blocks entry into mitosis [86–88]. Furthermore, an increase in IP_3 occurs before entry in mitosis and again at anaphase [4], consistent with a role for IP_3 in generating the calcium signals. On the other hand, some reports suggest that calcium transients are not required for progression of the cell cycle. For instance, high concentrations of calcium chelators abolish mitotic transients, but do not affect entry into mitosis [85]. Furthermore, in mouse embryos inhibition of IP_3Rs using 2-APB also abolishes calcium transients without affecting mitosis [85]. These data suggest that mitotic calcium signals are an epiphenomenon unrelated to cell cycle control.

The picture that emerges from these seemingly contradictory results is that measurements of intracellular calcium do not always support the idea that calcium transients are essential during mitosis. This led to the idea that mitotic calcium signals may occur in microdomains in many instances and that the larger transients may represent amplification of these small and localized calcium signals under some experimental conditions [89–91]. Some authors speculate that the calcium signals that control mitotic progression may occur in calcium microdomains so localized as to be undetectable in global calcium images. Thus, it is possible that undetectable calcium increases in microdomains initiate mitosis in reports which suggest that global calcium changes are not relevant for mitosis [42,76,77], although future studies are need the clarify this issue.

In the present study we have demonstrated that undifferentiated CSCs and adult MSCs exhibit IP_3R-mediated $[Ca^{2+}]_i$ oscillations, while in NPCs both IP_3Rs and RyRs mediate these oscillations. Interestingly calcium transients occur predominantly at the G_1/S transition suggesting a role for these calcium transients in progression of the cell cycle. This hypothesis is supported by the finding that IP_3R activation increases both the fraction of cells in G_2/M and cell proliferation rates. The present results give further insight into the mechanisms that control progression of the cell cycle in stem cells as distinct as CSCs and MSCs, describing a signaling mechanism that could promote rapid transition out of G_1 and therefore support the preservation of their pluripotent state.

Author disclosure statement

No competing financial interests exist.

Acknowledgments

This work was supported by Instituto Nacional de Ciência e Tecnologia de Nanomateriais de Carbono, CNPq (Conselho Nacional de Desenvolvimento Científico e Tecnológico), and Rede Mineira de Biotecnologia e Bioensaios (FAPEMIG, Fundação de Amparo à Pesquisa do Estado de Minas Gerais) Brazil. R.R.R, S.G. and L.O.L. is grateful for grants from CNPq, and FAPEMIG, Brazil. A.H.K. is grateful for grants from CNPq, and FAPESP.

Appendix A. Supplementary data

Supplementary data associated with this article can be found, in the online version, at doi:10.1016/j.bbamcr.2009.11.008.

References

[1] M.J. Berridge, Calcium signalling and cell proliferation, Bioessays 17 (1995) 491–500.
[2] L. Santella, The role of calcium in the cell cycle: facts and hypotheses, Biochem. Biophys. Res Commun. 244 (1998) 317–324.
[3] S.M. Ribeiro, H.A. Armelin, Ca2+ and Mg2+ requirements for growth are not concomitantly reduced during cell transformation, Mol. Cell. Biochem. 59 (1984) 173–181.
[4] B. Ciapa, D. Pesando, M. Wilding, M. Whitaker, Cell-cycle calcium transients driven by cyclic changes in inositol trisphosphate levels, Nature 368 (1994) 875–878.
[5] L. Munaron, S. Antoniotti, A. Fiorio Pla, D. Lovisolo, Blocking Ca2+ entry: a way to control cell proliferation, Curr. Med. Chem. 11 (2004) 1533–1543.
[6] R.A. Hickie, J.W. Wei, L.M. Blyth, D.Y. Wong, D.J. Klaassen, Cations and calmodulin in normal and neoplastic cell growth regulation, Can. J. Biochem. Cell Biol. = Rev. Can. Biochim. Biol. Cell. 61 (1983) 934–941.
[7] D.F. Owens, A.R. Kriegstein, Patterns of intracellular calcium fluctuation in precursor cells of the neocortical ventricular zone, J. Neurosci. 18 (1998) 5374–5388.
[8] T.A. Weissman, P.A. Riquelme, L. Ivic, A.C. Flint, A.R. Kriegstein, Calcium waves propagate through radial glial cells and modulate proliferation in the developing neocortex, Neuron 43 (2004) 647–661.
[9] E. Scemes, N. Duval, P. Meda, Reduced expression of P2Y1 receptors in connexin43-null mice alters calcium signaling and migration of neural progenitor cells, J. Neurosci. 23 (2003) 11444–11452.
[10] S. Kawano, S. Shoji, S. Ichinose, K. Yamagata, M. Tagami, M. Hiraoka, Characterization of Ca(2+) signaling pathways in human mesenchymal stem cells, Cell Calcium 32 (2002) 165–174.
[11] E. Yanagida, S. Shoji, Y. Hirayama, F. Yoshikawa, K. Otsu, H. Uematsu, M. Hiraoka, T. Furuichi, S. Kawano, Functional expression of Ca2+ signaling pathways in mouse embryonic stem cells, Cell Calcium 36 (2004) 135–146.
[12] M. Catsicas, V. Bonness, D. Becker, P. Mobbs, Spontaneous Ca2+ transients and their transmission in the developing chick retina, Curr. Biol. 8 (1998) 283–286.
[13] R.R. Resende, J.L. da Costa, A.H. Kihara, A. Adhikari, E. Lorencon, Intracellular Ca(2+) regulation during neuronal differentiation of murine embryonal carcinoma and mesenchymal stem cells, Stem Cells Dev in press (2008).
[14] R. Pearson, M. Catsicas, D. Becker, P. Mobbs, Purinergic and muscarinic modulation of the cell cycle and calcium signaling in the chick retinal ventricular zone, J. Neurosci. 22 (2002) 7569–7579.
[15] S.E. Webb, A.L. Miller, Calcium signalling during embryonic development, Nat. Rev. 4 (2003) 539–551.
[16] M.M. Syed, S. Lee, S. He, Z.J. Zhou, Spontaneous waves in the ventricular zone of developing mammalian retina, J. Neurophysiol. 91 (2004) 1999–2009.

[17] N. Kapur, G.A. Mignery, K. Banach, Cell cycle-dependent calcium oscillations in mouse embryonic stem cells, Am. J. Physiol. 292 (2007) C1510–1518.
[18] S. Geley, E. Kramer, C. Gieffers, J. Gannon, J.M. Peters, T. Hunt, Anaphase-promoting complex/cyclosome-dependent proteolysis of human cyclin A starts at the beginning of mitosis and is not subject to the spindle assembly checkpoint, J. Cell Biol. 153 (2001) 137–148.
[19] F. Santiago, E. Clark, S. Chong, C. Molina, F. Mozafari, R. Mahieux, M. Fujii, N. Azimi, F. Kashanchi, Transcriptional up-regulation of the cyclin D2 gene and acquisition of new cyclin-dependent kinase partners in human T-cell leukemia virus type 1r-infected cells, J. Virol. 73 (1999) 9917–9927.
[20] R.R. Resende, P. Majumder, K.N. Gomes, L.R. Britto, H. Ulrich, P19 embryonal carcinoma cells as in vitro model for studying purinergic receptor expression and modulation of *N*-methyl-D-aspartate-glutamate and acetylcholine receptors during neuronal differentiation, Neuroscience 146 (2007) 1169–1181.
[21] R.R. Resende, K.N. Gomes, A. Adhikari, L.R. Britto, H. Ulrich, Mechanism of acetylcholine-induced calcium signaling during neuronal differentiation of P19 embryonal carcinoma cells in vitro, Cell Calcium 43 (2008) 107–121.
[22] R.R. Resende, A.S. Alves, L.R. Britto, H. Ulrich, Role of acetylcholine receptors in proliferation and differentiation of P19 embryonal carcinoma cells, Exp. Cell Res. 314 (2008) 1429–1443.
[23] A. Adhikari, C.A. Penatti, R.R. Resende, H. Ulrich, L.R. Britto, E.J. Bechara, 5-Aminolevulinate and 4, 5-dioxovalerate ions decrease GABA(A) receptor density in neuronal cells, synaptosomes and rat brain, Brain Res. 1093 (2006) 95–104.
[24] J.R. Sanchez-Ramos, S. Song, S.G. Kamath, T. Zigova, A. Willing, F. Cardozo-Pelaez, T. Stedeford, M. Chopp, P.R. Sanberg, Expression of neural markers in human umbilical cord blood, Exp. Neurol. 171 (2001) 109–115.
[25] M. Suzuki, K. Muraki, Y. Imaizumi, M. Watanabe, Cyclopiazonic acid, an inhibitor of the sarcoplasmic reticulum Ca(2+)-pump, reduces Ca(2+)-dependent K+ currents in guinea-pig smooth muscle cells, Br. J. Pharmacol. 107 (1992) 134–140.
[26] O. Thastrup, P.J. Cullen, B.K. Drobak, M.R. Hanley, A.P. Dawson, Thapsigargin, a tumor promoter, discharges intracellular Ca2+ stores by specific inhibition of the endoplasmic reticulum Ca2(+)-ATPase, Proc. Natl. Acad. Sci. U. S. A. 87 (1990) 2466–2470.
[27] S.C. Taylor, C. Peers, Store-operated Ca2+ influx and voltage-gated Ca2+ channels coupled to exocytosis in pheochromocytoma (PC12) cells, J. Neurochem. 73 (1999) 874–880.
[28] J. Gafni, J.A. Munsch, T.H. Lam, M.C. Catlin, L.G. Costa, T.F. Molinski, I.N. Pessah, Xestospongins: potent membrane permeable blockers of the inositol 1,4,5-trisphosphate receptor, Neuron 19 (1997) 723–733.
[29] H.H. Kerschbaum, M.D. Cahalan, Single-channel recording of a store-operated Ca2+ channel in Jurkat T lymphocytes, Science (New York, NY) 283 (1999) 836–839.
[30] A. Zweifach, R.S. Lewis, Calcium-dependent potentiation of store-operated calcium channels in T lymphocytes, J. Gen. Physiol. 107 (1996) 597–610.
[31] H.H. Kerschbaum, M.D. Cahalan, Monovalent permeability, rectification, and ionic block of store-operated calcium channels in Jurkat T lymphocytes, J. Gen. Physiol. 111 (1998) 521–537.
[32] T. Maruyama, T. Kanaji, S. Nakade, T. Kanno, K. Mikoshiba, 2APB, 2-aminoethoxydiphenyl borate, a membrane-penetrable modulator of Ins(1,4,5)P3-induced Ca2+ release, J. Biochem. 122 (1997) 498–505.
[33] M. Fill, J.A. Copello, Ryanodine receptor calcium release channels, Physiol. Rev. 82 (2002) 893–922.
[34] A. Beck, R.Z. Nieden, H.P. Schneider, J.W. Deitmer, Calcium release from intracellular stores in rodent astrocytes and neurons in situ, Cell Calcium 35 (2004) 47–58.
[35] J. Meldolesi, Rapidly exchanging Ca2+ stores in neurons: molecular, structural and functional properties, Prog. Neurobiol. 65 (2001) 309–338.
[36] D.I. Yule, J.A. Williams, U73122 inhibits Ca2+ oscillations in response to cholecystokinin and carbachol but not to JMV-180 in rat pancreatic acinar cells, J. Biol. Chem. 267 (1992) 13830–13835.
[37] T.A. Ta, W. Feng, T.F. Molinski, I.N. Pessah, Hydroxylated xestospongins block inositol-1,4,5-trisphosphate-induced Ca2+ release and sensitize Ca2+-induced Ca2+ release mediated by ryanodine receptors, Mol. Pharmacol. 69 (2006) 532–538.
[38] D.O. Mak, S. McBride, J.K. Foskett, ATP-dependent adenophostin activation of inositol 1,4,5-trisphosphate receptor channel gating: kinetic implications for the durations of calcium puffs in cells, J. Gen. Physiol. 117 (2001) 299–314.
[39] M. Takahashi, K. Tanzawa, S. Takahashi, Adenophostins, newly discovered metabolites of Penicillium brevicompactum, act as potent agonists of the inositol 1,4,5-trisphosphate receptor, J. Biol. Chem. 269 (1994) 369–372.
[40] C. Clair, C. Chalumeau, T. Tordjmann, J. Poggioli, C. Erneux, G. Dupont, L. Combettes, Investigation of the roles of Ca(2+) and InsP(3) diffusion in the coordination of Ca(2+) signals between connected hepatocytes, J. Cell Sci. 114 (2001) 1999–2007.
[41] T. Krude, Mimosine arrests proliferating human cells before onset of DNA replication in a dose-dependent manner, Exp. Cell Res. 247 (1999) 148–159.
[42] C.Y. Gui, C. Jiang, H.Y. Xie, R.L. Qian, The apoptosis of HEL cells induced by hydroxyurea, Cell Res. 7 (1997) 91–97.
[43] I. Nishiyama, T. Fujii, Laminin-induced process outgrowth from isolated fetal rat C-cells, Exp. Cell Res. 198 (1992) 214–220.
[44] M.A. Jordan, D. Thrower, L. Wilson, Effects of vinblastine, podophyllotoxin and nocodazole on mitotic spindles. Implications for the role of microtubule dynamics in mitosis, J. Cell Sci. 102 (Pt. 3) (1992) 401–416.
[45] R.L. da Silva, R.R. Resende, H. Ulrich, Alternative splicing of P2X6 receptors in developing mouse brain and during in vitro neuronal differentiation, Exp. Physiol. 92 (2007) 139–145.
[46] N. Mackman, K. Brand, T.S. Edgington, Lipopolysaccharide-mediated transcriptional activation of the human tissue factor gene in THP-1 monocytic cells requires both activator protein 1 and nuclear factor kappa B binding sites, J. Exp. Med. 174 (1991) 1517–1526.
[47] M.M. Bradford, A rapid and sensitive method for the quantitation of microgram quantities of protein utilizing the principle of protein-dye binding, Anal. Biochem. 72 (1976) 248–254.
[48] E. Stead, J. White, R. Faast, S. Conn, S. Goldstone, J. Rathjen, U. Dhingra, P. Rathjen, D. Walker, S. Dalton, Pluripotent cell division cycles are driven by ectopic Cdk2, cyclin A/E and E2F activities, Oncogene 21 (2002) 8320–8333.
[49] R.R. Resende, L.R. Britto, H. Ulrich, Pharmacological properties of purinergic receptors and their effects on proliferation and induction of neuronal differentiation of P19 embryonal carcinoma cells, Int. J. Dev. Neurosci. 26 (2008) 763–777.
[50] R.L. Patterson, D. Boehning, S.H. Snyder, Inositol 1,4,5-trisphosphate receptors as signal integrators, Annu. Rev. Biochem. 73 (2004) 437–465.
[51] A. Verkhratsky, Endoplasmic reticulum calcium signaling in nerve cells, Biol. Res. 37 (2004) 693–699.
[52] M.J. Berridge, P. Lipp, M.D. Bootman, The versatility and universality of calcium signalling, Nat. Rev. 1 (2000) 11–21.
[53] M.J. Berridge, The endoplasmic reticulum: a multifunctional signaling organelle, Cell Calcium 32 (2002) 235–249.
[54] M. D'Ascenzo, R. Piacentini, P. Casalbore, M. Budoni, R. Pallini, G.B. Azzena, C. Grassi, Role of L-type Ca2+ channels in neural stem/progenitor cell differentiation, Eur. J. Neurosci. 23 (2006) 935–944.
[55] H.M. Yu, J. Wen, R. Wang, W.H. Shen, S. Duan, H.T. Yang, Critical role of type 2 ryanodine receptor in mediating activity-dependent neurogenesis from embryonic stem cells, Cell Calcium 43 (2008) 417–431.
[56] B.E. Ehrlich, E. Kaftan, S. Bezprozvannaya, I. Bezprozvanny, The pharmacology of intracellular Ca(2+)-release channels, Trends Pharmacol. Sci. 15 (1994) 145–149.
[57] Y.W. Peng, A.H. Sharp, S.H. Snyder, K.W. Yau, Localization of the inositol 1,4,5-trisphosphate receptor in synaptic terminals in the vertebrate retina, Neuron 6 (1991) 525–531.
[58] J. Gan, P.M. Iuvone, Depolarization and activation of dihydropyridine-sensitive Ca2+ channels stimulate inositol phosphate accumulation in photoreceptor-enriched chick retinal cell cultures, J. Neurochem. 68 (1997) 2300–2307.
[59] S. Osada, Y. Okano, S. Saji, Y. Nozawa, Spontaneous Ca2+ release from a caffeine and ryanodine-sensitive intracellular Ca2+ store in freshly prepared hepatocytes, Hepatology (Baltimore, Md.) 19 (1994) 514–517.
[60] D.D. Friel, R.W. Tsien, A caffeine- and ryanodine-sensitive Ca2+ store in bullfrog sympathetic neurones modulates effects of Ca2+ entry on [Ca2+]i, J. Physiol. 450 (1992) 217–246.
[61] L.L. Haak, L.S. Song, T.F. Molinski, I.N. Pessah, H. Cheng, J.T. Russell, Sparks and puffs in oligodendrocyte progenitors: cross talk between ryanodine receptors and inositol trisphosphate receptors, J. Neurosci. 21 (2001) 3860–3870.
[62] E.G. Harks, J.P. Camina, P.H. Peters, D.L. Ypey, W.J. Scheenen, E.J. van Zoelen, A.P. Theuvenet, Besides affecting intracellular calcium signaling, 2-APB reversibly blocks gap junctional coupling in confluent monolayers, thereby allowing measurement of single-cell membrane currents in undissociated cells, FASEB J. 17 (2003) 941–943.
[63] D. Bai, C. del Corsso, M. Srinivas, D.C. Spray, Block of specific gap junction channel subtypes by 2-aminoethoxydiphenyl borate (2-APB), J. Pharmacol. Exp. Ther. 319 (2006) 1452–1458.
[64] C.M. Peppiatt, T.J. Collins, L. Mackenzie, S.J. Conway, A.B. Holmes, M.D. Bootman, M.J. Berridge, J.T. Seo, H.L. Roderick, 2-Aminoethoxydiphenyl borate (2-APB) antagonises inositol 1,4,5-trisphosphate-induced calcium release, inhibits calcium pumps and has a use-dependent and slowly reversible action on store-operated calcium entry channels, Cell Calcium 34 (2003) 97–108.
[65] C.L. He, P. Damiani, J.B. Parys, R.A. Fissore, Calcium, calcium release receptors, and meiotic resumption in bovine oocytes, Biol. Reprod. 57 (1997) 1245–1255.
[66] L. Wang, K.L. White, W.A. Reed, K.D. Campbell, Dynamic changes to the inositol 1,4,5-trisphosphate and ryanodine receptors during maturation of bovine oocytes, Cloning Stem Cells 7 (2005) 306–320.
[67] L. Groigno, M. Whitaker, An anaphase calcium signal controls chromosome disjunction in early sea urchin embryos, Cell 92 (1998) 193–204.
[68] T. Hunter, J. Pines, Cyclins and cancer: II. Cyclin D and CDK inhibitors come of age, Cell 79 (1994) 573–582.
[69] D.O. Morgan, Principles of CDK regulation, Nature 374 (1995) 131–134.
[70] C.J. Sherr, G1 phase progression: cycling on cue, Cell 79 (1994) 551–555.
[71] I. Reynisdottir, K. Polyak, A. Iavarone, J. Massague, Kip/Cip and Ink4 Cdk inhibitors cooperate to induce cell cycle arrest in response to TGF-beta, Genes Dev. 9 (1995) 1831–1845.
[72] C.J. Sherr, J.M. Roberts, CDK inhibitors: positive and negative regulators of G1-phase progression, Genes Dev. 13 (1999) 1501–1512.
[73] M.J. Berridge, M.D. Bootman, H.L. Roderick, Calcium signalling: dynamics, homeostasis and remodelling, Nat. Rev. 4 (2003) 517–529.
[74] G.S. Williams, E.J. Molinelli, G.D. Smith, Modeling local and global intracellular calcium responses mediated by diffusely distributed inositol 1,4,5-trisphosphate receptors, J. Theor. Biol. 253 (2008) 170–188.
[75] T. Matsu-ura, T. Michikawa, T. Inoue, A. Miyawaki, M. Yoshida, K. Mikoshiba, Cytosolic inositol 1,4,5-trisphosphate dynamics during intracellular calcium oscillations in living cells, J. Cell Biol. 173 (2006) 755–765.
[76] L. Santella, E. Ercolano, G.A. Nusco, The cell cycle: a new entry in the field of Ca2+ signaling, Cell Mol. Life Sci. 62 (2005) 2405–2413.
[77] C.W. Taylor, A.J. Laude, IP3 receptors and their regulation by calmodulin and cytosolic Ca2+, Cell Calcium 32 (2002) 321–334.

[78] G. Halet, R. Tunwell, S.J. Parkinson, J. Carroll, Conventional PKCs regulate the temporal pattern of Ca2+ oscillations at fertilization in mouse eggs, J. Cell Biol. 164 (2004) 1033–1044.
[79] L. Jirmanova, M. Afanassieff, S. Gobert-Gosse, S. Markossian, P. Savatier, Differential contributions of ERK and PI3-kinase to the regulation of cyclin D1 expression and to the control of the G1/S transition in mouse embryonic stem cells, Oncogene 21 (2002) 5515–5528.
[80] J.S. Heo, Y.J. Lee, H.J. Han, EGF stimulates proliferation of mouse embryonic stem cells: involvement of Ca2+ influx and p44/42 MAPKs, Am. J. Physiol. 290 (2006) C123–C133.
[81] R.R. Resende, A. Adhikari, Cholinergic receptor pathways involved in apoptosis, cell proliferation and neuronal differentiation, Cell Commun. Signal. 7 (2009) 20.
[82] N. DeSouza, S. Reiken, K. Ondrias, Y.M. Yang, S. Matkovich, A.R. Marks, Protein kinase A and two phosphatases are components of the inositol 1,4,5-trisphosphate receptor macromolecular signaling complex, J. Biol. Chem. 277 (2002) 39397–39400.
[83] M. Hershfinkel, W.F. Silverman, I. Sekler, The zinc sensing receptor, a link between zinc and cell signaling, Mol. Med. (Cambridge, Mass.) 13 (2007) 331–336.
[84] N. Agell, O. Bachs, N. Rocamora, P. Villalonga, Modulation of the Ras/Raf/MEK/ERK pathway by Ca(2+), and calmodulin, Cell. Signal. 14 (2002) 649–654.
[85] G. FitzHarris, M. Larman, C. Richards, J. Carroll, An increase in [Ca2+]i is sufficient but not necessary for driving mitosis in early mouse embryos, J. Cell Sci. 118 (2005) 4563–4575.
[86] J. Twigg, R. Patel, M. Whitaker, Translational control of InsP3-induced chromatin condensation during the early cell cycles of sea urchin embryos, Nature 332 (1988) 366–369.
[87] R.A. Steinhardt, J. Alderton, Intracellular free calcium rise triggers nuclear envelope breakdown in the sea urchin embryo, Nature 332 (1988) 364–366.
[88] M. Wilding, E.M. Wright, R. Patel, G. Ellis-Davies, M. Whitaker, Local perinuclear calcium signals associated with mitosis-entry in early sea urchin embryos, J. Cell Biol. 135 (1996) 191–199.
[89] T. Kono, K.T. Jones, A. Bos-Mikich, D.G. Whittingham, J. Carroll, A cell cycle-associated change in Ca2+ releasing activity leads to the generation of Ca2+ transients in mouse embryos during the first mitotic division, J. Cell Biol. 132 (1996) 915–923.
[90] J.P. Kao, J.M. Alderton, R.Y. Tsien, R.A. Steinhardt, Active involvement of Ca2+ in mitotic progression of Swiss 3T3 fibroblasts, J. Cell Biol. 111 (1990) 183–196.
[91] P.K. Hepler, The role of calcium in cell division, Cell Calcium 16 (1994) 322–330.